AD_____

Award Number: W81XWH-04-1-0301

TITLE: Exploiting Novel Calcium-Mediated Apoptotic Processes for the Treatment of Human Breast Cancers with Elevated Nqo1 Levels

PRINCIPAL INVESTIGATOR: Melissa S. Bentle, Ph.D.,
David A. Boothman, Ph.D.

CONTRACTING ORGANIZATION: Case Western Reserve University
Cleveland, OH 44106-7285

REPORT DATE: March 2008

TYPE OF REPORT: Annual Summary

PREPARED FOR: U.S. Army Medical Research and Materiel Command
Fort Detrick, Maryland 21702-5012

REPORT DOCUMENTATION PAGE

Form Approved
OMB No. 0704-0188

1. REPORT DATE *(DD-MM-YYYY)*	**2. REPORT TYPE**	**3. DATES COVERED** *(From - To)*
01-03-2008	Annual Summary	6 FEB 2004 - 5 FEB 2008

4. TITLE AND SUBTITLE

Exploiting Novel Calcium-Mediated Apoptotic Processes for the Treatment of Human Breast Cancers with Elevated Nqo1 Levels

5a. CONTRACT NUMBER

5b. GRANT NUMBER
W81XWH-04-1-0301

5c. PROGRAM ELEMENT NUMBER

6. AUTHOR(S)
Melissa S. Bentle, Ph.D.; David A. Boothman, Ph.D.

E-Mail: melissa_srougi@med.unc.edu

5d. PROJECT NUMBER

5e. TASK NUMBER

5f. WORK UNIT NUMBER

7. PERFORMING ORGANIZATION NAME(S) AND ADDRESS(ES)

Case Western Reserve University
Cleveland, OH 44106-7285

8. PERFORMING ORGANIZATION REPORT NUMBER

9. SPONSORING / MONITORING AGENCY NAME(S) AND ADDRESS(ES)
U.S. Army Medical Research and Materiel Command
Fort Detrick, Maryland 21702-5012

10. SPONSOR/MONITOR'S ACRONYM(S)

11. SPONSOR/MONITOR'S REPORT NUMBER(S)

12. DISTRIBUTION / AVAILABILITY STATEMENT
Approved for Public Release; Distribution Unlimited

13. SUPPLEMENTARY NOTES

14. ABSTRACT
We demonstrate that the NQO1-dependent reduction of β-lap caused ROS generation, DNA breaks, and triggered calcium (Ca2+)-dependent γ-H2AX formation and PARP-1 hyperactivation. PARP-1 hyperactivation was an integral part of cell death caused by this compound, causing NAD+ and ATP losses that suppressed DNA repair and caused cell death. PARP-1 inhibition or intracellular Ca2+ chelation protected cells from β-lap-induced cell death. Similarly, hydrogen peroxide (H2O2), but not N-Methly-N'-nitro-N-nitrosoguanidine (MNNG), caused Ca2+-mediated PARP-1 hyperactivation and death. Thus, Ca2+-mediated PARP-1 hyperactivation and death. Thus, Ca2+ appears to be an important co-factor in PARP-1 hyperactivation after ROS-induced DNA damage. To further explore DNA repair as a resistance factor(s) that might impede cell death, we explored the contribution of DNA double-strand break (DSB) repair following β-lap exposure. B-Lap treatment resulted in the NQO1-dependent activation of the MRE11-Rad50-Nbs-1 (MRN) complex, as well as ATM Serine 1981, DNA-PKcs Theronine 2609, and Chk1 Serine 345 phosphorylation, indicative of ATR activation. These data suggested the simultaneous activation of both homologous recombination (HR) and non-homologous end joining (NHEJ) pathways. However, inhibition of NHEJ potentiated β-lap lethality.

15. SUBJECT TERMS
Calcium, non-caspase-mediated apoptosis, beta-lapachone, poly(ADP-ribose)polymerase-1, breast cancer, therapeutics, NQO1, DNA double-stranded breaks, non-homologous end joining

16. SECURITY CLASSIFICATION OF:			**17. LIMITATION OF ABSTRACT**	**18. NUMBER OF PAGES**	**19a. NAME OF RESPONSIBLE PERSON**
a. REPORT	**b. ABSTRACT**	**c. THIS PAGE**			USAMRMC
U	U	U	UU	35	**19b. TELEPHONE NUMBER** *(include area code)*

Table of Contents

Page

Introduction and Summary

β-Lapachone (β-Lap) is a naturally occurring 1,2 napthoquinone present in the bark of the South American Lapacho tree. Our lab has shown that β-lap elicits a unique cell death process in various human breast, lung and prostate cancers that have elevated levels of the two-electron oxidoreductase, NQO1 (E.C. 1.6.99.2) (1). B-Lap induces an NQO1-dependent form of cell death wherein poly (ADP-ribose) polymerase-1 (PARP-1) and p53 proteolytic cleavage fragments were noted (2), concomitant with μ-calpain activation (3). B-Lap-induced lethality and proteolysis were abrogated by dicoumarol (an NQO1 inhibitor), and were muted in cells deficient in NQO1 enzymatic activity (4). Restoration of NQO1 caused increased in drug sensitivity (1). In contrast to staurosporine (STS), global caspase inhibitors had little effect on β-lap lethality (1). β-Lap-mediated cell death exhibited classical features of apoptosis (e.g. DNA condensation, trypan blue exclusion, sub-G_0-G_1 cells, and terminal deoxynucleotidyl transferase-mediated dUTP nick end labeling (TUNEL)-positive cells). It was not, however, dependent on typical apoptotic mediators such as p53 or caspases (5). To date, the mechanisms responsible for this unique cell death have not been elucidated.

Body

1. Identification of the transporter(s) responsible for endoplasmic reticulum (ER) Ca^{2+} release after β-lap treatment

Data from our lab has demonstrated that within 3-10 min after β-lap treatment of NQO1 positive cells, release of intracellular Ca^{2+} from ER stores was observed, and that this early release was comparable to thapsigargin (Tg) exposures (6). Furthermore, BAPTA-AM blocked this early increase in cytosolic Ca^{2+} and overall cell death.

A number of attempts to recapitulate these data have been unsuccessful. Cells were examined for Ca^{2+} transients using identical methods as those described in Tagliarino, *et al*. MCF-7 cells loaded with the Ca^{2+} indicator dye fluo-4AM were observed by time-lapse confocal microscopy after treatment with 8 or 16 μM β-lap. Cells were observed for 0-45 min every 10 sec and no Ca^{2+} transients were observed. However, after β-lap treatment, if these same cells were treated with a positive control for Ca^{2+} release (e.g. ATP, ionomycin, or Tg) a robust transient was observed and monitored until fluorescence of the fluo-4AM reached near basal levels. These data indicate that the system was functioning properly and the cells retained the ability to mobilize Ca^{2+} after stimulation. Manipulation of the loading of the fluorescent Ca^{2+}indicator was attempted but no Ca^{2+} transient was observed by confocal microscopy after treatment of cells with 8 μM β-lap (Figure 1A and 1B).

To confirm the confocal studies, Ca^{2+} fluctuations were also monitored using fluorometry. MCF-7 cell populations of 3 million cells were examined at a time and loaded with fluo-4AM with and without the presence of extracellular Ca^{2+}. In either experimental situation, a rise in intracellular Ca^{2+} following 8 μM β-lap was not observed out to 20 min post-treatment (data not shown).

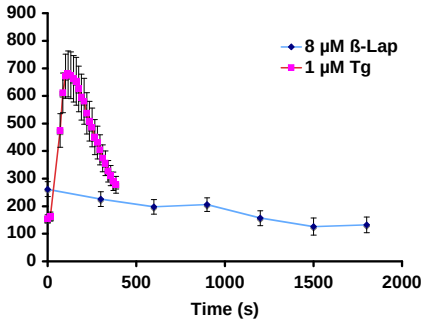

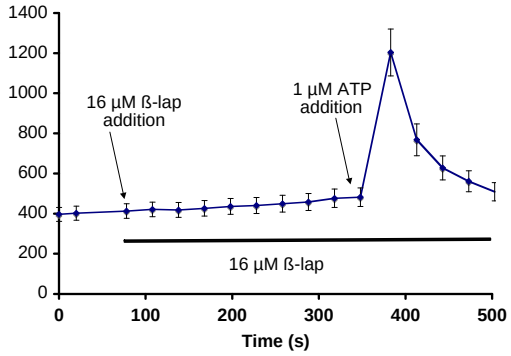

A. B.

Figure 1. **β-Lap does not cause an increase in cytosolic Ca^{2+} between 0-30 min**. MCF-7 cells were loaded with Ca^{2+} indicator dye Fluo-4AM for 30 min prior to treatment with 8 µM β-lap or 1 µM Tg at time 0 (A) or treated with 16 µM β-lap at ~100 s followed by 1 µM ATP addition after ~350 s (B). Fluo-4AM fluorescence was monitored using time-lapse confocal microscopy at 10 s intervals for the indicated times. Traces are the average of at least 60 cells and is representative of experiments performed in triplicate. For both A and B, the y-axes are Fluo-4AM fluorescence.

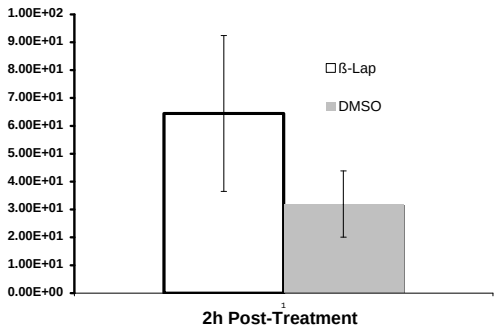

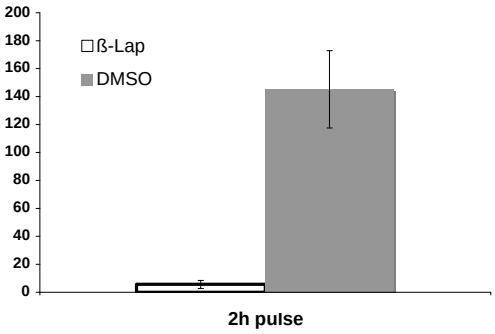

A. B.

Figure 2. **β-Lap causes a latent increase in cytosolic Ca^{2+} from ER stores.** MCF-7 cells were treated with 8 µM β-lap or vehicle alone for 2 hr. At which time cellular populations of 3 million were measured by fluorometry for increases in cytosolic (A) and thapsigargin releasable ER Ca^{2+} levels (B) using the Ca^{2+}-sensitive dye fluo-4AM. Results are the average of three independent experiments. The y axis are cytosolic [Ca^{2+}], nm and ER [Ca^{2+}], nm for (A) and (B) respectively.

Interestingly, an increase in cytosolic Ca^{2+} (Figure 2A) and a subsequent decrease in ER Ca^{2+} (Figure 2B) was observed 2 h after 8 µM β-lap treatment in MCF-7 cells compared to vehicle alone treated cells. This rise may be a consequence of the dysregulation of sarcoplasmic/endoplasmic reticulum Ca^{2+} ATPases (SERCA) activity due to PARP-1-mediated ATP loss. Therefore, the role of intranuclear Ca^{2+} in the early upstream signaling events of β-

lap-induced cell death and μ-calpain activation were then examined in relation to the modulation of PARP-1 activity (see below).

2. The role of PARP-1 in β-lap-induced cell death

*******For this section**,** please refer to the attached article entitled, "Calcium-dependent modulation of PARP-1 alters cellular metabolism and DNA repair" by Bentle *et al.* The Journal of Biological Chemistry 2006 November 3; 281(44):33684-33696.*******

β-Lap-induced PARP-1 hyperactivation alters NAD^+ and ATP pools causing cell death

PARP-1 hyperactivation can elicit a dramatic depletion of cellular NAD^+ levels and cause cell death in situations of extreme DNA damage or ischemia-reperfusion (7, 8). Treatment of MCF-7 cells with doses of β-lap ≥ 5 μM resulted in a rapid and >80% decrease in NAD^+ and ATP losses were attributable to PARP-1 hyperactivation, MCF-7 cells were pretreated for 2 h with PARP inhibitors 3-aminobenzamide (3-AB) or 3, 4-dihydro-5[4-(1-piperindinyl)butoxy]-1(2H)-isoquinoline (DPQ), prior to β-lap exposure. NAD^+ and ATP loss in β-lap-treated MCF-7 cells was partially abrogated by 3-AB or DPQ (Appended Figure 3A-C). Neither 3-AB nor DPQ (used at >2-fold doses than in the above experiments) altered NQO1 activity in *in vitro* enzyme assays. Finally, 3-AB did not affect β-lap-induced ROS formation.

To confirm these findings using PARP-1 inhibitors, we generated a MDA-MB-231 $NQO1^+$ and $NQO1^-$ cell line that had PARP-1 protein levels knocked-down (KD) using shRNA. 231-NQ+ PARP-1-shRNA cells had lower levels of PAR accumulation after β-lap treatment then 231-NQ+ non-silencing-shRNA (ns-shRNA) cells (Appended Figure 4B,C). Furthermore, KD of PARP-1 protein levels was sufficient to protect cells from β-lap-induced apoptosis (Appended Figure E).

Cumulatively, these data strongly suggest that Ca^{2+}-dependent PARP-1 hyperactivation caused NAD^+ and ATP loss in NQO1+ human breast cancer cell lines after β-lap treatment.

β-Lap causes NQO1-dependent DNA damage

Since PARP-1 hyperactivation typically requires DNA damage, we examined cells exposed to β-lap for the presence and magnitude of DNA strand breaks, by measuring γ-H2AX. H2AX contains a highly conserved serine residue (ser139), which is rapidly phosphorylated upon DNA damage (9). Significant γ-H2AX foci formation was observed by 30 min, similar to that seen 15 min following 5 Gy ionizing radiation (IR) (Appended Figure 5A,B). Total H2AX and α-tubulin levels remained constant for the duration of the β-lap exposure. These results were confirmed by confocal microscopy.

Previous experiments demonstrated that Ca^{2+} chelation blocked both β-lap-induced PARP-1 hyperactivation and cell death, we therefore, tested the effects of BAPTA-AM on γ-H2AX foci formation. Similar to the immunblot analyses and the PAR formation kinetics, β-lap-treated MCF-7 cells showed γ-H2AX foci at 30 min, with peak levels at 60 min. Importantly, β-lap-induced γ-H2AX foci formation was partially abrogated by BAPTA-AM addition, with few γ-H2AX foci noted in 30-60 min (Appended Figure 5C).

Ca^{2+} chelation allows for DNA repair after β-lap treatment

We postulated that the metabolism of β-lap by NQO1 would generate superoxide, peroxide, and other reactive oxygen species (ROS) (10). Since BAPTA-AM has moderate affinity for divalent cations other than Ca^{2+}, we explored the possibility that BAPTA-AM protected cells from DNA damage and subsequent cell death by interfering with Fenton chemistry. The oxidative state of MDA-MB-468-NQ+ cells was monitored after treatment with 4 μM β-lap in the presence or absence of 5 μM BAPTA-AM. β-Lap treatment caused an ~65% rise in disulfide glutathione (GSSG) levels, that persisted during drug exposure (Appended Figure 6A). Addition of BAPTA-AM did not alter the kinetics or levels of GSSG formation after β-lap exposure (Appended Figure 6A). These data suggest that the protective effects of BAPTA-AM on β-lap-treated NQO1+ cells were not due to interference with β-lap-induced ROS formation. Similar results were found in MCF-7 and 231-NQ+ cells.

To assess the effects of Ca^{2+} on DNA damage and repair, β-lap-treated MCF-7 cells were analyzed by alkaline comet assays to monitor total DNA strand breaks with or without BAPTA-AM addition. β-Lap-treated cells exhibited significant DNA strand breakage by 30 min, resembling the positive control (H_2O_2), and after 30 min, β-lap-induced DNA damage exceeded those levels. Cells pretreated with BAPTA-AM exhibited far less DNA damage compared to β-lap alone and their repair of DNA damage correlated well with their ability to survive (Appended Figure 6B *left panel*).

We then examined the kinetics of repair in MCF-7 cells following 2 h β-lap exposures with or without BAPTA-AM addition. After β-lap exposure, DNA damage persisted and gradually increased over time, indicative of inhibition of DNA repair and consistent with the rapid drop in NAD^+ and ATP levels. In contrast, cells treated with β-lap and BAPTA-AM exhibited less DNA damage at 2 h, and showed a time-dependent recovery (Appended Figure 6B *right panel*). Thus, NQO1-mediated metabolism of β-lap leads to the generation of ROS and subsequent DNA damage that hyperactivates PARP-1. Ca^{2+}-dependent PARP-1 hyperactivation drives the loss of NAD^+ and ATP levels, which suppresses DNA repair and survival.

In addition, we noted that the mechanism of β-lap-induced cell death had many parallels to that of H_2O_2. These findings are discussed in further detail in the appended manuscript (Appended Figure 7).

3. <u>To elucidate the role of single- and double-strand break repair following β-lap exposure</u>

For this section, please refer to the attached manuscript entitled, “Non-homologous end-joining is essential for cellular resistance to the novel anti-tumor agent, β-lapachone” by Bentle *et al.,* Cancer Research 2007 July 15; 67(14):6936-6945.

The MRN complex is activated after β-lap exposure

We had previously demonstrated that the NQO1-mediated metabolism of β-lap caused ROS and DNA damage (11). We wanted to further elucidate what DNA double-strand break (DSB) repair pathways were activated in response to β-lap treatment. We therefore examined the potential recruitment of the MRE11-Rad50-Nbs1 (MRN) complex which is a known indicator of DNA DSB (12). MCF-7 cells were treated with β-lap for various times and stained with antibodies complementary to MRE11, Rad50, and phosphorylated Ser343 Nbs-1 (Nbs-1-p). We

observed increases in the nuclear localization of all three proteins of the MRN complex suggesting the activation of DSB repair (Appended Figure 1A,B).

ATM and DNA-PK activation after β-lap treatment is dose-dependent

Because the MRN complex was recruited after exposure to β-lap, we examined cells for the activation of ATM, a HR-associated PI3K as well as DNA-PKcs, a NHEJ protein. β-Lap-treated MCF-7 cells exhibited a dose-dependent activation of both ATM and DNA-PKcs as monitored by their activated phosphorylated forms (ATM-pSer1981 as well as DNA-PKcs-pThr2609) (Appended Figure 2A,B). These data suggested that both HR and NHEJ are activated after β-lap exposure, but the predominant DNA repair pathway activated is NHEJ (Appended Figure 2C).

NHEJ is necessary for β-lap-induced cell death

Due to the robust activation of DNA-PK after β-lap exposure, we examined the consequences of its inhibition on lethality. Glioblastoma cell lines, MO59K, containing DNA-PKcs and MO59J cells lacking DNA-PKcs were utilized (13). DNA-PKcs-deficient MO59J cells were significantly more sensitive to β-lap than their DNA-PKcs-proficient counterparts, MO59K cells (Appended Figure 3A). To further assess DNA-PKcs functionality, we pretreated both MO59J and MO59K cells with a DNA-PKcs selective inhibitor Nu7026 before β-lap exposure. Nu7026 had little effect on β-lap-induced cell death in the MO59J cells because they lack DNA-PKcs activity. In contrast, Nu7026 significantly sensitized MO59K cells to β-lap (Appended Figure 3B).

To confirm that DNA-PK was essential in resistance to β-lap-induced cell death, MCF-7 cells were treated with sublethal doses of β-lap with or without pretreatment and cotreatment with Nu7026 and relative survival was determined. β-lap doses less than 2 μM had little to no toxicity alone, however, when MCF-7 cells were pretreated with Nu7026 and β-lap lethality was potentiated (Appended Figure 3C). The lethal events that were observed were mainly due to inhibition of DNA-PKcs rather than ATM (Appended Figure 3D).

We previously showed that β-lap-induced cell death was mediated by PARP-1-hyperactivation (11). Because a deficiency in DNA-PKcs potentiated β-lap-induced cell death, we examined whether NHEJ inhibition was accompanied by PARP-1 hyperactivation at sublethal does of β-lap. We noted PARP-1 hyperactivation in cells lacking DNA-PKcs after β-lap treatment (Appended Figure 3E).

HR-associated PI3K ATM is not necessary for β-lap-induced cell death

Since we had observed ATM autophosphorylation after β-lap treatment, we wanted to determine whether loss of ATM would alter β-lap-mediated lethality. Isogenic $NQO1^{+}$ human immortalized fibroblasts from A-T patients deficient in ATM ($ATM^{-/-}$) or proficient via ectopic ATM expression ($ATM^{+/+}$) were used (14). $ATM^{+/+}$ or $ATM^{-/-}$ exposed to β-lap exhibited no observable differences in lethality as compared to mock-treated cells (Appended Figure 4A). Furthermore, MCF-7 cells treated with sublethal doses of β-lap in the presence or absence of the ATM

inhibitor Ku55933 showed no differences in lethality suggesting that ATM does not play a dominant role in the repair of β-lap-induced DNA damage (Appended Figure 4B).

β-lap causes ATR activation and single-stranded DNA breaks (SSBs)

HR can also be mediated by ATR, which is recruited to single-stranded DNA regions, arising due to replication fork arrest or during the processing of bulky lesions, such as UV photoproducts (15). We reasoned that β-lap could generate ROS-induced SSBs, causing replication fork arrest. We therefore, examined whether ATR activation occurred in response to β-lap by using a set of stable cell lines derived from human osteosarcoma U2OS cells. These cells are wild-type for p53, have an intact G_1 DNA-damage checkpoint, and allow the doxycycline-inducible expression of either wild-type (WT) ATR or a dominant-negative (kinase-dead, KD) point mutant (16). ATR activation was confirmed by monitoring Chk1-pSer345 levels in WT U2OS cells after exposure to UVC or β-lap (Appended Figure 5A). Chk1-pSer345 was muted in U2OS KD-ATR cells after either UVC or β-lap exposures (Appended Figure 5A).

To confirm our findings that HR was not necessary for β-lap-induced cell death, we treated MCF-7 cells with AAI, an inhibitor of both ATM and ATR, before β-lap exposure. Inhibition of both enzymes was not sufficient to enhance β-lap-mediated cytotoxicity compared with the 80% enhancement observed after inhibition of DNA-PKcs (Appended Figure 3C and 4C). These data indicate that ATR signaling is activated after β-lap exposure, but that it is not a predominant factor required for survival.

β-lap-induced ATR activation and PARP-1 hyperactivation suggested that this compound caused extensive SSBs, whereas MRN, ATM, and DNA-PK foci formation indicated delayed DSB formation. Neutral and alkaline comet assays were done to elucidate the type(s) of breaks created in NQO1-proficient human cancer cells after β-lap expsosure. Lethal doses of β-lap resulted in significant total DNA breaks, occurring immediately after drug exposure at levels surpassing breaks created after 500 μM H_2O_2 (Appended Figure 5C). Interestingly, when cells were analyzed under neutral conditions, little to no DSBs were detected, in contrast to etoposide (ETO) treatment (Appended Figure 5C). These studies suggested that the majority of DNA damage caused by the NQO1-mediated metabolism of β-lap was SSBs, consistent with the genesis of “long-lived”damaging species (e.g. H_2O_2).

Key Research Accomplishments

- β-Lap treatment does not cause ER Ca^{2+} release 0-45 min after drug exposure in MCF-7 cells
- β-Lap-induced PARP-1 hyperactivation depletes NAD^+ and ATP pools causing cell death
- β-Lap causes NQO1-dependent DNA damage
- Ca^{2+} chelation allows for DNA repair after β-Lap treatment
- β-Lap causes activation of both HR and NHEJ DNA DSB repair pathways
- NHEJ, however, seems to be the primary mechanism by which cells repair β-Lap-induced DNA damage, as NHEJ inhibitors/deficient cell lines potentiate sub-lethal doses of β-Lap

Reportable Outcomes

- Publications:
  - **Bentle, M.S.,** Reinicke, K.E., Bey, E.A., Spitz, D.R., and Boothman, D.A. Calcium-Dependent Modulation of PARP-1 Alters Cellular Metabolism and DNA Repair. (2006) The Journal of Biological Chemistry, 281(44), 33684-33696.
  - **Bentle, M.S.,** Bey, E.A., Dong, Y., Reinicke, K.E., and Boothman, D.A. New Tricks for Old Drugs: The Anticarcinogenic Potential of DNA Repair Inhibitors. (2006) The Journal of Molecular Histology, 37(5-7), 203-218.
  - **Bentle, M.S.,** Dong, Y., Reinicke, K.E., Bey, E.A., and Boothman, D.A. Non-Homologous End Joining is Essential for Cellular Resistance to the Novel Cancer Chemotherapeutic Agent β-Lapachone. (2007) Cancer Research, 67(14), 6936-6945.
  - Bey, E.A., **Bentle, M.S.,** Reinicke, K.E., Dong, Y., and Boothman, D.A. A Novel NQO1-and PARP-1-Mediated Cell Death Pathway Induced in Non-Small Cell Lung Cancer Cells by β-Lapachone. (2007) Proceedings of the National Academy of Science USA, 104(28) 11832-11837.
  - **Bentle, M.S.** Involvement of single- and double-stranded break repair processes in β-lapachone-induced cell death. Published Thesis. August, 2007.
- Meeting Abstracts and Presentations:
  - **Bentle, M.S.** and Boothman, D.A. Calcium-mediated poly(ADP-ribose)polymerase-1 hyperactivation in β-Lapachone-induced programmed necrosis. Dept. of Pharmacology Retreat, Case Western Reserve University, Cleveland, OH 2002-06.
  - **Bentle, M.S.** and Boothman, D.A. Calcium-mediated poly(ADP-ribose)polymerase-1 hyperactivation in β-Lapachone-induced programmed necrosis. Biomedical Graduate Student Symposium, Case Western Reserve University, Cleveland, OH April 2002-06.
  - **Bentle, M.S.** and Boothman, D.A. Calcium-mediated poly(ADP-ribose)polymerase-1 hyperactivation in β-Lapachone-induced programmed necrosis. Dept. of Defense, Era of Hope Conference, Philadelphia PA, June 2005
  - **Bentle, M.S.** and Boothman, D.A. Calcium-mediated poly(ADP-ribose)polymerase-1 hyperactivation in β-Lapachone-induced programmed necrosis. Keystone Symposium, Metabolomics: from Metabolism to Apoptosis. Snowbird, UT, April 2006.
- Awards:
  - Outstanding Poster Award, Dept. of Pharmacology, Case Western Reserve University, Cleveland, OH for presentation entitled, “The mechanisms of β-lapachone-induced cell death” October, 2005
  - The Vance Lemmon Poster Award, Biomedical Graduate Student Symposium, Case Western Reserve University, Cleveland, OH for presentation entitled, “The role of calcium release and poly(ADP-ribose)polymerase-1 activation in β-lapachone-mediated cell death” April, 2005
  - The Marcus Singer Poster Award, Biomedical Graduate Student Symposium, Case Western Reserve University, Cleveland, OH for presentation entitled, “Calcium-Dependent Modulation of PARP-1 Alters Cellular Metabolism and DNA Repair” April, 2006

- Associate Member, American Association for Cancer Research
- Ph.D. degree in Pharmacology awarded, Case Western Reserve University, August 2007
- NIH Post-Doctoral Fellow in the laboratory of Dr. Keith Burridge, Lineberger Comprehensive Cancer Center, University of North Carolina at Chapel Hill, September 2007

Conclusions

We demonstrate that the NQO1-dependent reduction of β-lap caused ROS generation, DNA breaks, and triggered calcium (Ca^{2+})-dependent γ-H2AX formation and PARP-1 hyperactivation. PARP-1 hyperactivation was an integral part of cell death caused by this compound, causing NAD^+ and ATP losses that suppressed DNA repair and caused cell death. PARP-1 inhibition or intracellular Ca^{2+} chelation protected cells from β-lap-induced cell death. Similarly, hydrogen peroxide (H_2O_2), but not *N*-Methly-*N'*-nitro-*N*-nitrosoguanidine (MNNG), caused Ca^{2+}-mediated PARP-1 hyperactivation and death. Thus, Ca^{2+}-mediated PARP-1 hyperactivation and death. Thus, Ca^{2+} appears to be an important co-factor in PARP-1 hyperactivation after ROS-induced DNA damage.

To further explore DNA repair as a resistance factor(s) that might impede cell death, we explored the contribution of DNA double-strand break (DSB) repair following β-lap exposure. B-Lap treatment resulted in the NQO1-dependent activation of the MRE11-Rad50-Nbs-1 (MRN) complex, as well as ATM Serine 1981, DNA-PKcs Theronine 2609, and Chk1 Serine 345 phosphorylation, indicative of ATR activation. These data suggested the simultaneous activation of both homologous recombination (HR) and non-homologous end joining (NHEJ) pathways. However, inhibition of NHEJ potentiated β-lap lethality.

These data provide insight into the mechanism by which β-lap kills cancer cells expressing endogenously elevated NQO1 levels. Furthermore, targeting NHEJ to enhance the therapeutic efficacy of β-lap alone, or in combination with other agents that are also potentiated by DSB repair inhibitors, is warranted.

References

1. Pink, J. J., Planchon, S. M., Tagliarino, C., Varnes, M. E., Siegel, D., and Boothman, D. A. NAD(P)H:Quinone oxidoreductase activity is the principal determinant of beta-lapachone cytotoxicity. J Biol Chem, *275:* 5416-5424, 2000.
2. Pink, J. J., Wuerzberger-Davis, S., Tagliarino, C., Planchon, S. M., Yang, X., Froelich, C. J., and Boothman, D. A. Activation of a cysteine protease in MCF-7 and T47D breast cancer cells during beta-lapachone-mediated apoptosis. Exp Cell Res, *255:* 144-155, 2000.
3. Tagliarino, C., Pink, J. J., Reinicke, K. E., Simmers, S. M., Wuerzberger-Davis, S. M., and Boothman, D. A. Mu-calpain activation in beta-lapachone-mediated apoptosis. Cancer Biol Ther, *2:* 141-152, 2003.
4. Ough, M., Lewis, A., Bey, E. A., Gao, J., Ritchie, J. M., Bornmann, W., Boothman, D. A., Oberley, L. W., and Cullen, J. J. Efficacy of beta-lapachone in pancreatic cancer treatment: exploiting the novel, therapeutic target NQO1. Cancer Biol Ther, *4:* 95-102, 2005.

5. Wuerzberger, S. M., Pink, J. J., Planchon, S. M., Byers, K. L., Bornmann, W. G., and Boothman, D. A. Induction of apoptosis in MCF-7:WS8 breast cancer cells by beta-lapachone. Cancer Res, *58:* 1876-1885, 1998.
6. Tagliarino, C., Pink, J. J., Dubyak, G. R., Nieminen, A. L., and Boothman, D. A. Calcium is a key signaling molecule in beta-lapachone-mediated cell death. J Biol Chem, *276:* 19150-19159, 2001.
7. Szabo, C. and Dawson, V. L. Role of poly(ADP-ribose) synthetase in inflammation and ischaemia-reperfusion. Trends Pharmacol Sci, *19:* 287-298, 1998.
8. Pieper, A. A., Verma, A., Zhang, J., and Snyder, S. H. Poly (ADP-ribose) polymerase, nitric oxide and cell death. Trends Pharmacol Sci, *20:* 171-181, 1999.
9. Rogakou, E. P., Pilch, D. R., Orr, A. H., Ivanova, V. S., and Bonner, W. M. DNA double-stranded breaks induce histone H2AX phosphorylation on serine 139. J Biol Chem, *273:* 5858-5868, 1998.
10. Reinicke, K. E., Bey, E. A., Bentle, M. S., Pink, J. J., Ingalls, S. T., Hoppel, C. L., Misico, R. I., Arzac, G. M., Burton, G., Bornmann, W. G., Sutton, D., Gao, J., and Boothman, D. A. Development of beta-lapachone prodrugs for therapy against human cancer cells with elevated NAD(P)H:quinone oxidoreductase 1 levels. Clin Cancer Res, *11:* 3055-3064, 2005.
11. Bentle, M. S., Reinicke, K. E., Bey, E. A., Spitz, D. R., and Boothman, D. A. Calcium-dependent modulation of poly(ADP-ribose) polymerase-1 alters cellular metabolism and DNA repair. J Biol Chem, *281:* 33684-33696, 2006.
12. Paull, T. T., Rogakou, E. P., Yamazaki, V., Kirchgessner, C. U., Gellert, M., and Bonner, W. M. A critical role for histone H2AX in recruitment of repair factors to nuclear foci after DNA damage. Curr Biol, *10:* 886-895, 2000.
13. Allalunis-Turner, M. J., Barron, G. M., Day, R. S., 3rd, Dobler, K. D., and Mirzayans, R. Isolation of two cell lines from a human malignant glioma specimen differing in sensitivity to radiation and chemotherapeutic drugs. Radiat Res, *134:* 349-354, 1993.
14. Ziv, Y., Bar-Shira, A., Pecker, I., Russell, P., Jorgensen, T. J., Tsarfati, I., and Shiloh, Y. Recombinant ATM protein complements the cellular A-T phenotype. Oncogene, *15:* 159-167, 1997.
15. Cortez, D., Guntuku, S., Qin, J., and Elledge, S. J. ATR and ATRIP: partners in checkpoint signaling. Science, *294:* 1713-1716, 2001.
16. Nghiem, P., Park, P. K., Kim Ys, Y. S., Desai, B. N., and Schreiber, S. L. ATR is not required for p53 activation but synergizes with p53 in the replication checkpoint. J Biol Chem, *277:* 4428-4434, 2002.

THE JOURNAL OF BIOLOGICAL CHEMISTRY VOL. 281, NO. 44, pp. 33684–33696, November 3, 2006

Calcium-dependent Modulation of Poly(ADP-ribose) Polymerase-1 Alters Cellular Metabolism and DNA Repair*[S]

Received for publication, April 17, 2006, and in revised form, August 17, 2006 Published, JBC Papers in Press, August 17, 2006, DOI 10.1074/jbc.M603678200

Melissa S. Bentle[‡], Kathryn E. Reinicke[§], Erik A. Bey[¶], Douglas R. Spitz[‖], and David A. Boothman[‡§¶1]

From the Departments of [‡]Pharmacology and [§]Biochemistry, Case Western Reserve University, Cleveland, Ohio 44106, the [¶]Department of Pharmacology, Laboratory of Molecular Stress Responses, and the Simmons Comprehensive Cancer Center, University of Texas Southwestern Medical Center, Dallas, Texas 75390, and the [‖]Department of Radiation Oncology, Free Radical and Radiation Biology Program, Holden Comprehensive Cancer Center, University of Iowa, Iowa City, Iowa 52242

After genotoxic stress poly(ADP-ribose) polymerase-1 (PARP-1) can be hyperactivated, causing (ADP-ribosyl)ation of nuclear proteins (including itself), resulting in NAD^+ and ATP depletion and cell death. Mechanisms of PARP-1-mediated cell death and downstream proteolysis remain enigmatic. β-lapachone (β-lap) is the first chemotherapeutic agent to elicit a Ca^{2+}-mediated cell death by PARP-1 hyperactivation at clinically relevent doses in cancer cells expressing elevated NAD(P)H:quinone oxidoreductase 1 (NQO1) levels. β-lap induces the generation of NQO1-dependent reactive oxygen species (ROS), DNA breaks, and triggers Ca^{2+}-dependent γ-H2AX formation and PARP-1 hyperactivation. Subsequent NAD^+ and ATP losses suppress DNA repair and cause cell death. Reduction of PARP-1 activity or Ca^{2+} chelation protects cells. Interestingly, Ca^{2+} chelation abrogates hydrogen peroxide (H_2O_2), but not *N*-Methyl-*N*′-nitro-*N*-nitrosoguanidine (MNNG)-induced PARP-1 hyperactivation and cell death. Thus, Ca^{2+} appears to be an important co-factor in PARP-1 hyperactivation after ROS-induced DNA damage, which alters cellular metabolism and DNA repair.

Alterations in the initiation and regulation of caspase-mediated apoptosis are associated with an array of pathological disease states, including chemotherapy resistance in cancer (1). Therefore, elucidating mechanisms that initiate non-caspase-mediated cell death are crucial for the development and use of novel anticancer agents.

A growing number of chemotherapeutic approaches focus on targeting specific DNA repair enzymes. In particular, inhibitors of poly(ADP-ribose) polymerase-1 (PARP-1)[2] that sensitize cells to DNA-damaging agents are under extensive investigation (2). PARP-1 functions as a DNA damage sensor that responds to both single- and/or double-strand DNA breaks (SSBs, DSBs), facilitating DNA repair and cell survival. After binding to DNA breaks, PARP-1 converts β-NAD^+ (NAD^+) into polymers of branched or linear poly(ADP-ribose) units (PAR) and attaches them to various nuclear acceptor proteins, including XRCC1, histones, and PARP-1 for its autoregulation (3). However, in response to extensive DNA damage, PARP-1 can be hyperactivated, eliciting rapid cellular NAD^+ and ATP pool depletion. PARP-1-mediated NAD^+ and ATP losses have affects on mitochondrial function by decreasing the levels of pyruvate and NADH. Loss of mitochondrial membrane potential (MMP) ensues, causing caspase-independent cell death by as yet unknown mechanisms (3). PARP-1 hyperactivation was documented in the cellular response to trauma, such as ischemia-reperfusion, myocardial infarction, and reactive oxygen species (ROS)-induced injury (3). In each case, inhibition of PARP-1 was necessary for the long-term survival of damaged cells (4).

β-lapachone (β-lap) elicits a unique cell death process in various human breast, lung, and prostate cancers that have elevated levels of the two-electron oxidoreductase, NAD(P)H:quinone oxidoreductase 1 (NQO1) (EC 1.6.99.2) (5). β-lap induces an NQO1-dependent form of cell death wherein PARP-1 and p53 proteolytic cleavage fragments were noted (6), concomitant with μ-calpain activation (7). β-lap-induced lethality and proteolysis were abrogated by dicoumarol (an NQO1 inhibitor), and were muted in cells deficient in NQO1

* This work was supported in part by National Institutes of Health/NCI Grant 1R01CA10279201 (to D. A. B.), 1R01CA100045 (to D. R. S.), CWRU Core Grants P30CA43703 and P30CA43703-12, as well as Department of Defense Breast Cancer Program Predoctoral Fellowships, W81XWH-04-1-0301 and W81XWH-05-1-0248 (to M. S. B. and K. E. R.), respectively. This is manuscript CSCN 001 from the Cell Stress and Cancer Nanomedicine program in the Simmons Comprehensive Cancer Center at the University of Texas Southwestern Medical Center at Dallas. The costs of publication of this article were defrayed in part by the payment of page charges. This article must therefore be hereby marked "*advertisement*" in accordance with 18 U.S.C. Section 1734 solely to indicate this fact.

[S] The on-line version of this article (available at http://www.jbc.org) contains supplemental experimental procedures, Figs. S1–S5, and Table S1.

[1] To whom correspondence should be addressed: Dept. of Pharmacology, Laboratory of Molecular Stress Responses, and the Simmons Comprehensive Cancer Center, UT Southwestern Medical Center, 5323 Harry Hines Blvd, Dallas, TX 75390. Tel.: 214-648-9255; Fax: 214-648-0264; E-mail: David.Boothman@UTSouthwestern.edu.

[2] The abbreviations used are: PARP-1, poly(ADP-ribose) polymerase-1; β-lap, β-lapachone (3,4-dihydro-2,2-dimethyl-2*H*-naphthol[1,2b]pyran-5,6-dione); ROS, reactive oxygen species; H_2O_2, hydrogen peroxide; MNNG, *N*-methyl-*N*′-nitro-*N*-nitrosoguanidine; SSBs/DSBs, single/double-stranded DNA breaks; PAR, poly(ADP-ribose); MMP, mitochondrial membrane potential; NQO1, NAD(P)H:quinone oxidoreductase 1; STS, staurosporine; TUNEL, terminal deoxynucleotidyl transferase-mediated dUTP nick-end labeling; BAPTA-AM, (1,2-bis-(2-aminophenoxy)ethane-*N*,*N*,*N*′,*N*′-tetraacetic acid tetra-(acetoxymethyl ester)); Me_2SO, dimethyl sulfoxide; DIC, dicoumarol; 3-AB, 3-aminobenzamide; DPQ, (3,4-dihydro-5[4-(1-piperindinyl)butoxy]-1(2H)-isoquinoline); DCF, 6-carboxy-2′7′-dichlorodihydrofluorescin diacetate, di(acetoxymethyl ester); 231, MDA-MB-231; ns-shRNA, non-silencing shRNA; ER, endoplasmic reticulum; 231-NQ−, MDA-MB-231-NQO1-negative; 231-NQ+, MDA-MB-231-NQO1-positive; PARG, poly(ADP-ribose) glycohydrolase; IR, ionizing radiation; Topo, topoisomerase; MOMP, mitochondrial outer membrane permeabilization; PP2A, protein phosphatase 2A; PMCA, plasma membrane Ca^{2+}-ATPase; SERCA, sarcoplasmic/endoplasmic reticulum ATPase; TRMP, transient receptor potential-melastatin-like; AIF, apoptosis-inducing factor.

enzymatic activity (5). Restoration of NQO1 caused increases in drug sensitivity (5). In contrast to staurosporine (STS), global caspase inhibitors had little effect on β-lap lethality (5). β-lap-mediated cell death exhibited classical features of apoptosis (*e.g.* DNA condensation, trypan blue exclusion, sub-G_0-G_1 cells, and terminal deoxynucleotidyl transferase-mediated dUTP nick-end labeling (TUNEL)-positive cells). β-lap cell death was not, however, dependent on typical apoptotic mediators, such as p53 or caspases (8). To date, the mechanisms responsible for the initiation of this unique cell death have not been delineated.

We report that β-lap induces an NQO1-dependent, PARP-1-mediated cell death pathway involving changes in cellular metabolism leading to cell death. NQO1-dependent reduction of β-lap results in a futile redox cycle between the parent β-lap molecule and its hydroquinone form (5), wherein ROS generation causes extensive DNA damage, H2AX phosphorylation (γ-H2AX) and PARP-1 hyperactivation. Drastic decreases in NAD^+ and ATP pools, in turn, inhibit DNA repair and accelerate cell death. In addition, chelation of intracellular Ca^{2+} by 1,2-bis-(2-aminophenoxy)ethane-*N*,*N*,*N*′,*N*′-tetraacetic acid tetra-acetoxymethyl ester (BAPTA-AM) abrogates β-lap-induced: (i) γ-H2AX formation, (ii) PARP-1 hyperactivation, (iii) atypical PARP-1 and p53 proteolysis, and (iv) cytotoxicity without affecting NQO1-dependent ROS production. A similar Ca^{2+}-sensitive cell death is observed after hydrogen peroxide (H_2O_2) exposure. Interestingly, *N*-methyl-*N*′-nitro-*N*-nitrosoguanidine (MNNG)-induced PARP-1 hyperactivation is not sensitive to BAPTA-AM. These data support a critical role for Ca^{2+} as a regulator of cellular metabolism in response to ROS-induced DNA damage.

EXPERIMENTAL PROCEDURES

Reagents—β-lap was synthesized by Dr. William G. Bornmann (MD Anderson), dissolved in dimethyl sulfoxide (Me_2SO) at 40 mM, and the concentration verified by spectrophotometric analyses (8). β-lap stocks were stored at −80 °C. Hoechst 33258, 3-aminobenzamide (3-AB), dicoumarol (DIC), H_2O_2, STS, and MNNG were obtained from Sigma. BAPTA-AM was dissolved in Me_2SO and used at 5 μM unless otherwise stated. DPQ (3,4-dihydro-5[4-(1-piperindinyl)butoxy]-1(2*H*)-isoquinoline) was dissolved in Me_2SO and used at 20 μM. DPQ and BAPTA-AM were obtained from Calbiochem (La Jolla, CA). Z-VAD-fmk was obtained from Enzyme Systems Products (Dublin, CA), diluted in Me_2SO and used at 50 μM. DCF was dissolved in Me_2SO and used at 5 μM to monitor ROS formation. DCF was obtained from Molecular Probes (Eugene, OR).

Cell Culture—Human MCF-7 and MDA-MB-468-NQ+ breast cancer cells were maintained and used as described (5). Human MDA-MB-231 (231) breast cancer cells that contain a 609C>T polymorphism in NQO1 (9) and are deficient in enzyme activity, were obtained from the American Type Culture Collection (Manassas, VA). Cells were stably transfected with a CMV-driven NQO1 cDNA or the pcDNA3 vector alone as described (5). All cells were grown in high glucose-containing RPMI 1640 tissue culture medium containing 5% fetal bovine serum, 2 mM L-glutamine, 100 units/ml penicillin, and 100 mg/ml streptomycin at 37 °C in a 5% CO_2, 95% air humidified atmosphere (6). 231-NQO1+ (NQ+) and −NQO1 (NQ−) cells were maintained in medium containing 400 μg/ml geneticin (8), but all experiments were performed without selection. All tissue culture components were purchased from Invitrogen (Carlsbad, CA) unless otherwise stated. All cells were routinely tested and found free of mycoplasma contamination.

PARP-1 Knockdown—A puromycin-selectable-pSHAG-MAGIC2 retroviral vector containing a short hairpin small interfering RNA against PARP-1 (PARP-1-shRNA) and a non-silencing sequence (ns-shRNA) control were used to infect both NQ+ and NQ− 231 cells (Open Biosystems, Huntsville, AL). Cells were then selected and grown in 0.5 μg/ml puromycin and screened for PARP-1 protein expression and NQO1 enzymatic activity.

Relative Survival Assays—Relative survival assays were performed as previously described (5). MCF-7 cells were pretreated or not with BAPTA-AM (5 μM, 30 min) then treated with or without 2-h pulses of β-lap at the doses indicated, in the presence or absence of 40 μM dicoumarol. In some experiments, cells were exposed to 5 μM β-lap followed by delayed ($t = 0–2$ h) addition of 5 μM BAPTA-AM. After drug addition, media were removed and drug-free media added. Cells were then allowed to grow for an additional 6 days and relative survival, based on DNA content (Hoechst 33258 staining), was determined (5). Prior studies using β-lap showed that relative survival assays correlated directly with colony forming ability assays (5). Data were expressed as treated/control (T/C) from separate triplicate experiments (means, ± S.E.), and comparisons analyzed using a two-tailed Student's *t* test for paired samples.

Immunoblotting and Confocal Microscopy—Western blots were prepared as previously described (8). α-PARP (sc-8007) and α-p53 (DO-1) antibodies were utilized at dilutions of 1:1000 (Santa Cruz Biotechnology). The α-PAR antibody was used at 1:2000 dilution (BD-Pharmingen, San Jose, CA). Antibodies to total levels of H2AX or γ-H2AX were used at dilutions of 1:100–1:500 and purchased from Bethyl Laboratories (Montgomery, TX) and Upstate (Charlottesville, VA), respectively. An NQO1 antibody was generated and used directly for immunoblot analyses in medium containing 10% fetal bovine serum, 1× phosphate-buffered saline, and 0.2% Tween 20 (10).

Confocal microscopy was performed as previously described (7). Cells were fixed in methanol/acetone (1:1) and incubated with α-PAR (10H; Alexis, San Diego, CA) or α-γ-H2AX (Trevigen, Gaithersburg, MD) for 2 h at room temperature. Nuclei were visualized by Hoechst 33258 staining at a 1:3000 dilution. Confocal images were collected at 488 nm excitation from a krypton/argon laser using a Zeiss LSM 510 confocal microscope (Thornwood, NY). Images were representative of experiments performed at least four times. The number of PAR-positive cells and γ-H2AX foci/cell were quantified by counting 60 or more cells from four independent experiments (means ± S.E.).

Formation of ROS was monitored by the conversion of non-fluorescent 6-carboxy-2′7′-dichlorodihydrofluorescin diacetate, di(acetoxymethyl ester) to fluorescent 6-carboxy-2′,7′-dichlorofluorescein diacetate di(acetoxymethyl ester) (DCF) as previously described (11, 12). Briefly, MCF-7 cells were seeded

at 2–3 × 10^5 cells in 35-mm glass bottom Petri dishes (MatTek Corp., Ashland, MA) and allowed to attach overnight. Cells were loaded with 5 μM DCF in media for 30 min at 37 °C. After loading, cells were washed twice with phosphate-buffered saline, and incubated for an additional 20 min at 37 °C to allow for dye de-esterification. Confocal images of DCF fluorescence were collected using 488-nm excitation from an argon/krypton laser, 560-nm dichroic mirror, and a 500–550 nm band pass filter. Three basal images were collected before drug addition (5–8 μM β-lap, +5 μM BAPTA-AM or 40 μM dicoumarol). Subsequent images were taken after the indicated treatments at 15-s intervals and similar results were found at 37 °C or rm. temp. BAPTA-AM was co-loaded with DCF where indicated. Mean pixel intensities were determined in regions of interest for at least 40 individual cells at each time point. Shown are representative traces of at least three independent experiments (means ± S.E.).

Single Cell Gel Electrophoresis (Alkaline Comet) Assays—DNA damage was assessed after different drug treatments by evaluating DNA "comet" tail area and migration distance (13). MCF-7 cells were pretreated with BAPTA-AM (5 μM, 30 min) or Me_2SO (1:1000 dilution), and then exposed to H_2O_2 (500 μM, 1 h), β-lap (4 μM, various times), or vehicle alone, and harvested at various times. Cell suspensions (3 × 10^5/ml cold PBS) were mixed with 1% low melting temperature agarose (1:10 (v/v)) at 37 °C and immediately transferred onto a CometSlide™ (Trevigen). After solidifying (30 min at 4 °C), slides were submerged in prechilled lysis buffer (2.5 M NaCl, 100 mM EDTA pH 10, 10 mM Tris Base, 1% sodium lauryl sarcosinate, and 1% Triton X-100) at 4 °C for 45 min, incubated in alkaline unwinding solution (300 mM NaOH, and 1 mM EDTA) for 45 min at room temperature and washed twice (5 min) in neutral 1× TBE (89.2 mM Tris Base, 89 mM boric acid, and 2.5 mM EDTA disodium salt). Damaged and undamaged nuclear DNA was then separated by electrophoresis in 1× TBE for 10 min at 1 V/cm, fixed in 70% ethanol, and stained using SYBR-green (Trevigen). Comets were visualized using an Olympus fluorescence microscope (Melville, NY), and images captured using a digital camera. Images were analyzed using ImageJ software (14, 15) and comet tail length was calculated as the distance between the end of nuclei heads and the end of each tail. Tail moments were defined as the product of the %DNA in each tail, and the distance between the mean of the head and tail distributions in Equation 1,

$$\%DNA_{(tail)} = TA \times TAI \times 100/(TA \times TAI) + [HA \times HAI] \quad \text{(Eq. 1)}$$

where TA is the tail area, TAI is the tail area intensity, HA is the head area, and HAI is the head area intensity. Importantly, tail moment and tail area calculations yielded similar experimental results. Each datum point represented the average of 100 cells ± S.E., and data are representative of experiments performed three times.

Determination of NAD^+ and ATP Levels—Intracellular NAD^+ levels were measured as described (16) with modification. Briefly, cells were seeded at 1 × 10^6 and allowed to attach overnight. Cells were pretreated for 2 h with 3-AB (25 mM), DPQ (20 μM), BAPTA-AM (5 μM), or Me_2SO and then exposed to β-lap (2–20 μM) for the indicated times. Cell extracts were prepared in 0.5 M perchloric acid, neutralized (1 M KOH, 0.33 M KH_2PO_4/K_2HPO_4 (pH 7.5)), and centrifuged to remove $KClO_4$ precipitates. Supernatants or NAD^+ standards were incubated 4:1 (v/v) for 20 min at 37 °C with NAD^+ reaction mixture as described (17). Measurements from extracts were taken at an absorbance of 570 nm and intracellular NAD^+ levels were normalized to 1 × 10^6 cells. Data were expressed as %NAD^+ ± S.E., for T/C samples from nine individual experiments.

ATP levels were analyzed using a luciferase-based bioluminescence assay as described (18). Data were graphed as means ± S.E. of experiments performed at least three times. Results were compared using the two-tailed Student's *t* test for paired samples.

NQO1 Enzyme Activity Assays—NQO1 enzymatic assays were performed as described (19) using cytochrome *c* (practical grade, Sigma) in Tris-HCl buffer (50 mM, pH 7.5). NADH (200 μM) was the immediate electron donor, and menadione (10 μM) the electron acceptor. Changes in absorbance were monitored using a Beckman DU 640 spectrophotometer (Beckman Coulter, Fullerton, CA). Dicoumarol (10 μM) inhibitable NQO1 levels were calculated as nmol of cytochrome *c* reduced/min/μg protein based on initial rate of change in absorbance at 550 nm and an extinction coefficient for cytochrome *c* of 21.1 nmol/liter/cm (20). Results were expressed as means ± S.E. of three or more separate experiments.

Flow Cytometry and Apoptotic Measurements—Flow cytometric analyses of TUNEL-positive cells were performed as described using APO-DIRECT™ (BD Pharmingen) (5). Samples were analyzed in an EPICS Elite ESP flow cytometer using an air-cooled argon laser at 488 nm, 15 milliwatt (Beckman Coulter Electronics, Miami, FL) and Elite acquisition software. Experiments were performed a minimum of five times, and data expressed as means ± S.E. Statistical analyses were performed using a two-tailed Student's *t* test for paired samples.

Glutathione Measurements—Disulfide glutathione and total glutathione (GSH + GSSG) levels were determined using a spectrophotometric recycling assay (21, 22). Following indicated treatments, pellets were thawed and whole cell homogenates prepared as described (21, 22). Data were expressed as the %GSSG normalized to protein content, as measured using the method of Lowry *et al.* (23). Shown are means ± S.E. for experiments performed at least three times.

RESULTS

Time and Ca^{2+} Dependence of β-lap-induced Cell Death—To elucidate the signaling events required for β-lap-induced cell death, log-phase human MCF-7 breast cancer cells, with high levels of endogenous NQO1 activity, were tested for their sensitivities to various concentrations of β-lap at various times. The purpose of these experiments was to determine the minimal time of β-lap exposure required to kill the entire cell population. Cells exposed to doses of ≤3 μM β-lap required ≥4 h to elicit cell death, whereas 2 h exposures of β-lap at ≥4 μM killed all MCF-7 cells (Fig. 1*A*).

Prior data from our laboratory demonstrated that Ca^{2+} was released within 2–5 min from endoplasmic reticulum (ER)

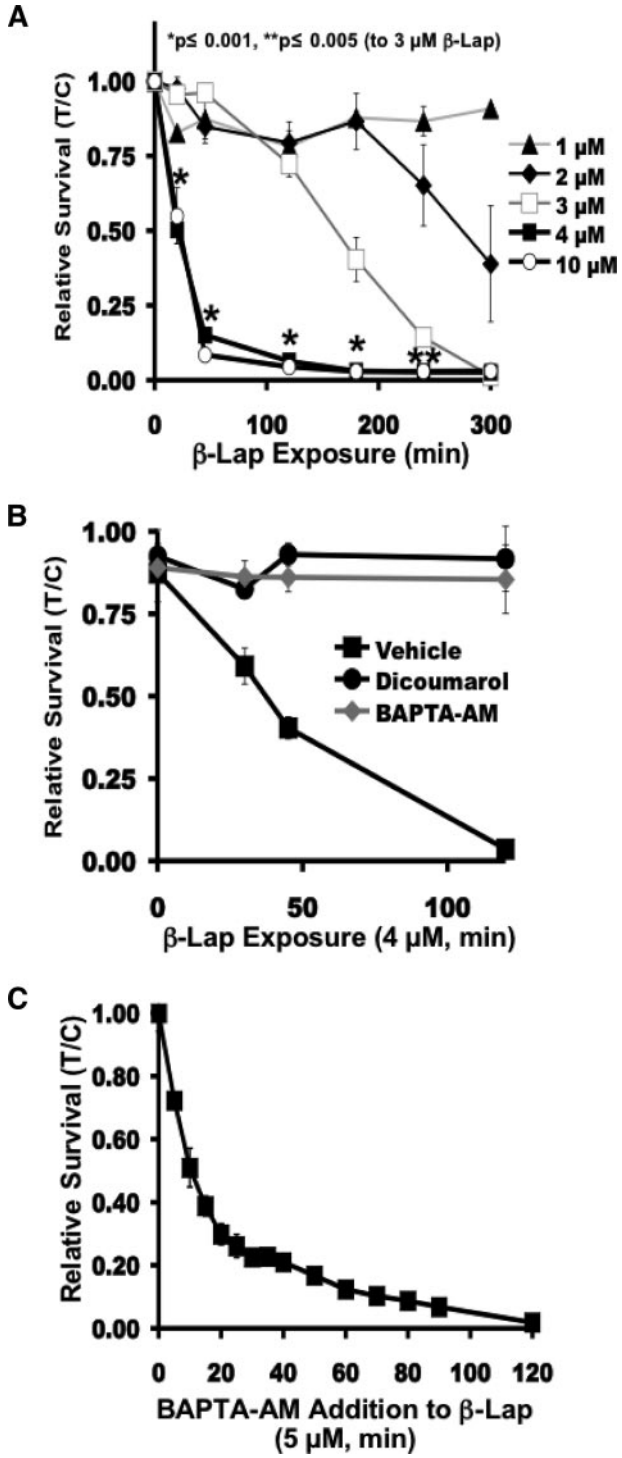

FIGURE 1. **β-lap-induced cell death is time- and Ca^{2+}-dependent.** *A–C,* cell death was examined using relative survival assays in NQO1+ MCF-7 cells. *A,* cells were exposed to various doses of β-lap for different lengths of time to determine the minimal exposure time required for cell death. After drug exposure, media were removed and drug-free media added. Cells were then allowed to grow for an additional 6 days and relative survival, based on DNA content was determined by Hoechst 33258 staining as described under "Experimental Procedures." Student's *t* test for paired samples, experimental group compared with 3 μM β-lap (*, $p \leq 0.001$; **, $p \leq 0.005$). Prior studies using β-lap showed that relative survival assays directly correlated with colony forming ability. *B,* relative survival assays using MCF-7 cells treated with 4 μM β-lap alone, or in combination with 40 μM dicoumarol or 5 μM BAPTA-AM. *C,* MCF-7 cells were treated with 5 μM β-lap at $t = 0$. BAPTA-AM (5 μM) was then added to β-lap-treated cells at various times afterwards as indicated.

Ca^{2+} stores after β-lap treatment (24), suggesting that this was a required initiating factor in β-lap-induced cell death (24). To test this, MCF-7 cells were pretreated with the intracellular Ca^{2+} chelator BAPTA-AM (5 μM, 30 min), then exposed to 4 μM β-lap for various times (Fig. 1*B*). Under these conditions, we previously demonstrated that BAPTA-AM pretreatment was sufficient to block the rise in cytosolic Ca^{2+} caused by β-lap treatment (24). BAPTA-AM abrogated β-lap-induced cytotoxicity and nuclear condensation (Fig. 1*B* and supplemental Fig. S1*A*). To determine the kinetics of Ca^{2+}-dependent cell death, MCF-7 cells were treated with 5 μM β-lap, and 5 μM BAPTA-AM was added at various times thereafter, up to 2 h. A time-dependent decrease in survival was observed with delayed addition of BAPTA-AM (Fig. 1*C*), indicating that Ca^{2+} release was a necessary event, occurring before cells were committed to death. Abrogation of β-lap cytotoxicity by BAPTA-AM was equivalent to that noted with NQO1 inhibition by dicoumarol (Fig. 1*B*). Addition of BAPTA-AM also prevented β-lap-induced, atypical proteolysis (*e.g.* ~60 kDa PARP-1 and p53 cleavage fragments), in a manner as effective as dicoumarol (supplemental Fig. S1*B*, *lanes 3* and *4*). Interestingly, Z-VAD-fmk (50 μM), a pan-caspase inhibitor, did not block atypical PARP-1 and p53 proteolysis in β-lap-treated MCF-7 cells (*lane 7*). As expected, Z-VAD-fmk inhibited STS (1 μM)-induced caspase-mediated proteolysis (25). However, BAPTA-AM did not affect STS-induced apoptotic proteolysis (supplemental Fig. S1*C*). These data, in conjunction with our prior data showing β-lap-induced ER Ca^{2+} release (24), support a role for Ca^{2+} in the initiation of cell death induced by this drug.

PARP-1 Hyperactivation after β-lap Treatment Is NQO1-dependent and BAPTA-AM-sensitive—Because β-lap-induced cell death was accompanied by a ≥80% loss of ATP within 1 h (24), we suspected PARP-1 hyperactivation played a role in the mode of action for this drug. To investigate this, we generated 231 NQO1-proficient (231-NQ+) cells that are sensitive to β-lap (LD_{50}: ~1.5 μM), after a 2-h pulse, and compared these cells to vector alone, 231 NQO1-deficient (231-NQ-) cells, that are resistant to the drug (LD_{50}: 17.5 μM). Only β-lap-treated, 231-NQ+ cells exhibited an increase in PAR-modified proteins, mostly PARP-1, consistent with the role of PARP-1 as the predominant poly(ADP-ribosyl)ated species. This response peaked ~30 min during β-lap exposure (Fig. 2*A*). In contrast, treatment of 231-NQ- cells with equal or significantly higher doses of β-lap did not induce PAR accumulation (data not shown). In contrast, both 231-NQ+ and 231-NQ- cells hyperactivated PARP-1 in response to H_2O_2. The NQO1-dependence of PARP-1 hyperactivation after β-lap exposure was confirmed in a number of other cell lines (*e.g.* breast, prostate, and lung cancers) that have elevated NQO1 activity demonstrating that the responses to β-lap were not cell type-specific. In all cases, dicoumarol suppressed β-lap-induced PAR formation (supplemental Fig. S2, *A–C*).

We then examined a possible connection between the involvement of Ca^{2+} in lethality and PARP-1 hyperactivation. MCF-7 cells were pretreated with 5 μM BAPTA-AM, then exposed to 5 μM β-lap for the indicated times (Fig. 2*B*). The kinetics of PAR accumulation were faster in MCF-7 cells than in 231-NQ+ cells, (10 min *versus* 20 min Figs. 2, *B* and *A*,

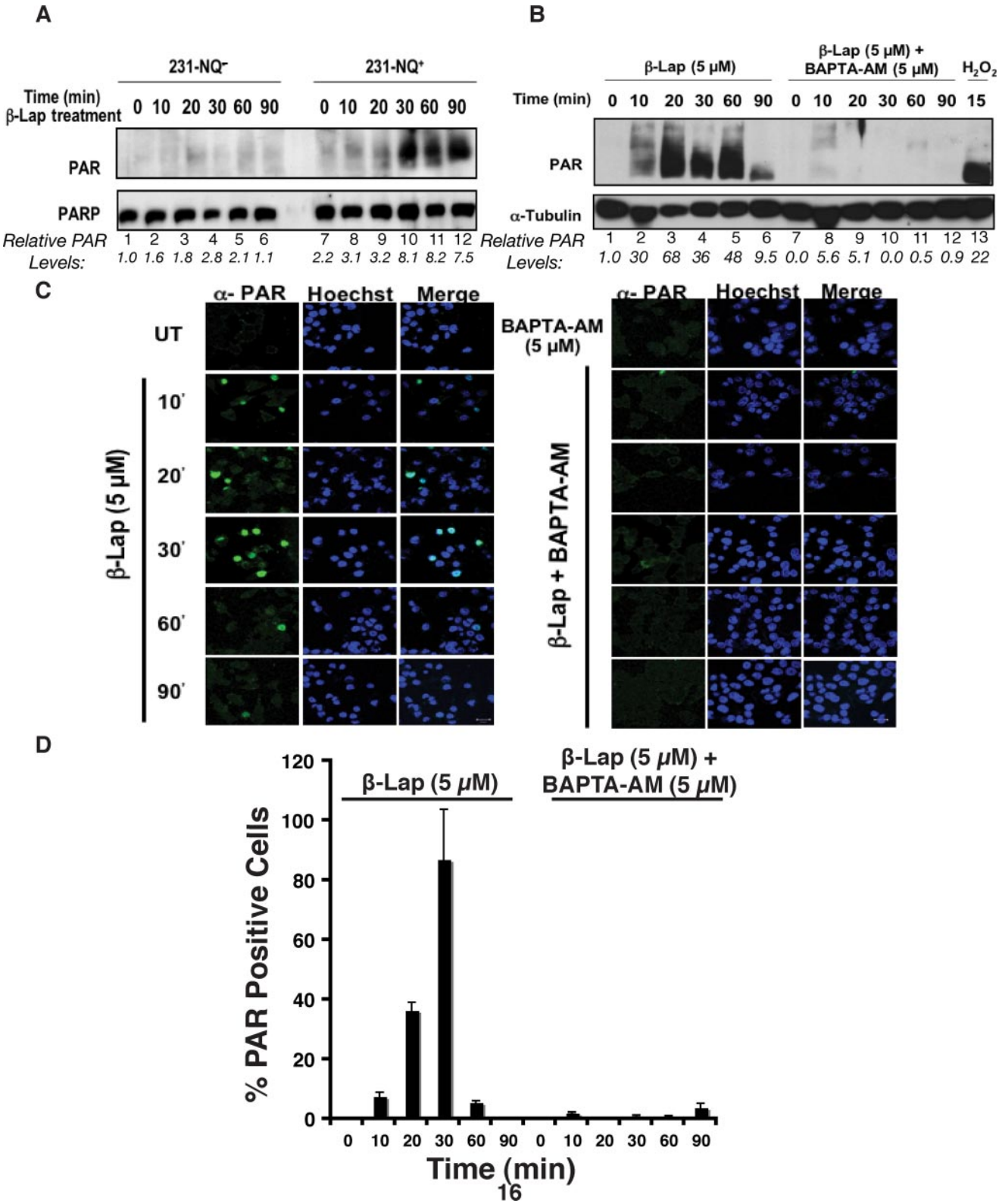

FIGURE 2. **β-lap induces NQO1- and Ca^{2+}-dependent PARP-1 hyperactivation.** *A*, immunoblots of PAR formation as a measure of PARP-1 hyperactivation, and steady-state PARP-1 protein levels from whole cell extracts of isogenic 231-NQ+ and 231-NQ− cells treated with 6 μM β-lap for 10–90 min. Relative PAR levels were calculated by densitometric analyses by NIH ImageJ using PARP loading controls wherein controls were set to 1.0. *B*, immunoblots of PAR formation and steady state α-tubulin expression in extracts from MCF-7 cells treated with β-lap or H_2O_2 (2 mM, control for PARP-1 hyperactivation). Other cells were pretreated with BAPTA-AM with or without β-lap (5 μM). Samples were harvested at the indicated times. Relative PAR levels were calculated by densitometric analyses by NIH ImageJ using α-tubulin loading controls wherein controls were set to 1.0. *C*, assessment of PARP-1 hyperactivation, measured by PAR formation, in MCF-7 cells treated with β-lap alone or in cells pretreated with BAPTA-AM for 30 min prior to β-lap exposure. PAR formation was visualized using confocal microscopy. *D*, quantified percentages of PAR-positive cells from confocal microscopy analyses of at least 60 cells from four independent experiments (means ± S.E.).

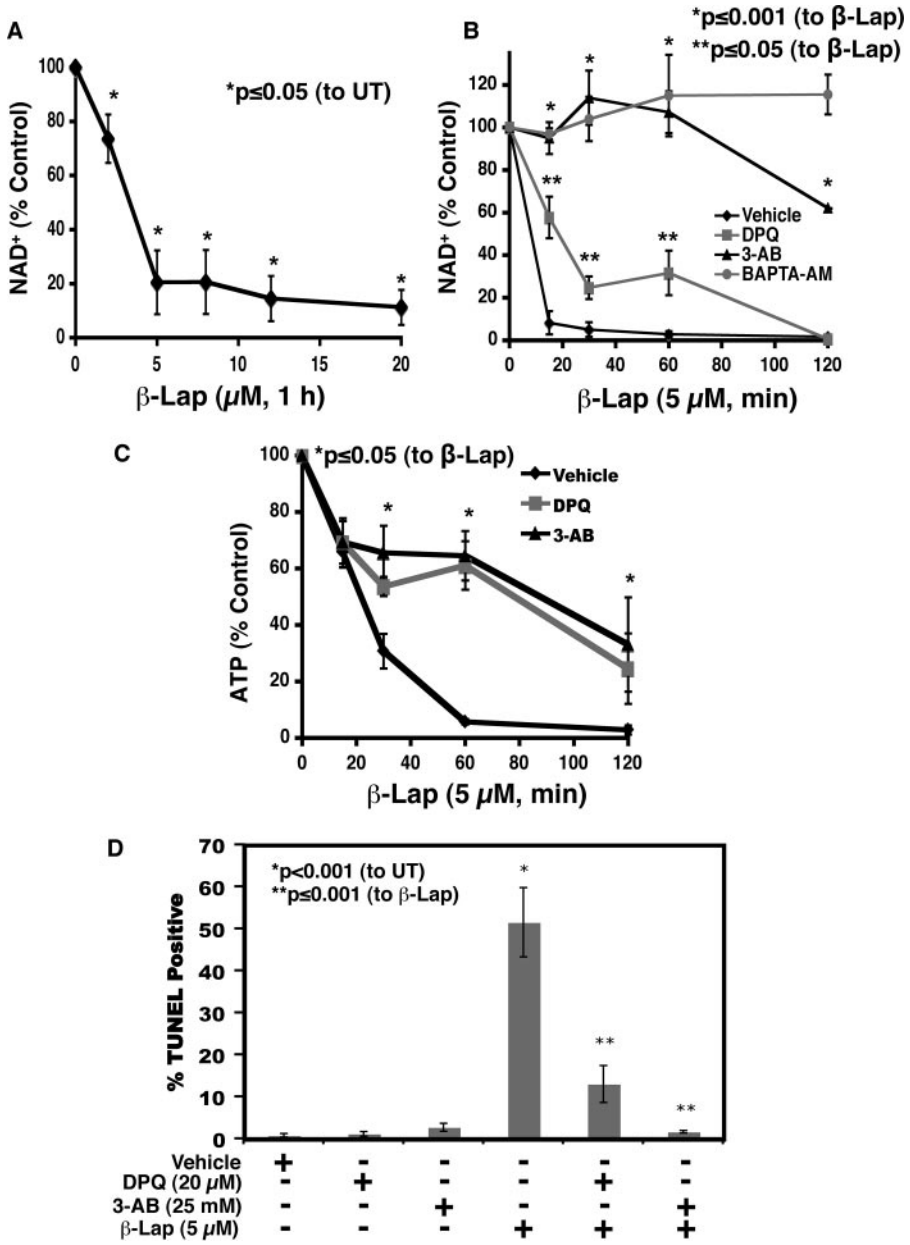

FIGURE 3. **PARP-1-dependent NAD^+ and ATP pool depletion leads to cell death after β-lap exposure in MCF-7 cells.** *A* and *B*, NAD^+ pool depletion occurs immediately after β-lap treatment in MCF-7 cells. *A*, MCF-7 cells were exposed to varying concentrations of β-lap for 1 h, or *B*, 5 μM β-lap alone with or without pre- and co-treatment of PARP inhibitors, (20 μM DPQ or 25 mM 3-AB) or 5 μM BAPTA-AM for various times and harvested for NAD^+ content. Student's *t* test for paired samples, comparing experimental groups containing β-lap + 3-AB or DPQ *versus* β-lap alone are indicated (*, $p \leq 0.001$; **, $p \leq 0.05$, respectively). *C*, intracellular ATP levels were monitored using a luciferase-based bioluminescence assay in MCF-7 cells treated with β-lap, or in cells pre- and co-treated with 20 μM DPQ, or 25 mM 3-AB 2 h prior to β-lap addition. Differences were compared using two-tailed Student's *t* test. Groups having *, $p \leq 0.05$ values compared with β-lap alone are indicated. *D*, apoptotic DNA fragmentation was assessed using TUNEL assays in β-lap-exposed, log-phase MCF-7 cells with or without pre- and co-treatment with DPQ or 3-AB.

respectively), consistent with higher NQO1 levels in MCF-7 cells. PAR levels decreased after 90 min, corresponding to auto-(ADP-ribosyl)ation of PARP-1, and efficient PAR hydrolysis by poly(ADP-ribose) glycohydrolase (PARG) (26). Interestingly, BAPTA-AM pretreatment abrogated PARP-1 hyperactivation induced by β-lap (Fig. 2*B*) as confirmed by confocal microscopy (Fig. 2*C*). Robust and extensive poly(ADP-ribosyl)ation occurred within 30 min (87% ± 17 PAR-positive cells) of drug exposure and dissipated between 60–90 min (Fig. 2, *C* and *D*). However, in the presence of BAPTA-AM PAR accumulation in β-lap-treated MCF-7 cells was prevented (Fig. 2, *C* and *D*). To determine the global nature of this response, other cancer cell lines such as NQO1+ PC-3 human prostate cancer cells were examined and similar responses noted (supplemental Fig. S2*D*). Collectively, these data suggested a role for Ca^{2+} in the modulation of PARP-1 hyperactivation after β-lap exposure.

β-lap-induced PARP-1 Hyperactivation Alters Cellular Energy Dynamics Causing Cell Death—PARP-1 hyperactivation can elicit depletion of cellular NAD^+ levels and cause cell death in situations of extreme DNA damage or ischemia-reperfusion (27, 28). Treatment of MCF-7 cells with doses of β-lap ≥5 μM resulted in decreases (>80%) in NAD^+ and ATP levels 1 h during treatment (Fig. 3, *A–C*). To determine if NAD^+ and ATP losses were attributable to PARP-1 hyperactivation, MCF-7 cells were pretreated for 2 h with PARP inhibitors (*i.e.* 3-AB or DPQ), prior to 5 μM β-lap exposure. Similar to pretreatment with BAPTA-AM, NAD^+ and ATP losses in β-lap-treated MCF-7 cells were abrogated by 3-AB or DPQ (Fig. 3, *B* and *C*). 3-AB was more effective at preventing nucleotide loss than DPQ presumably because it has two distinct modes of PARP-1 inhibition, preventing NAD^+ binding to the catalytic site and competing with the PARP-1 DNA binding domain (29), whereas DPQ is a competitive inhibitor of NAD^+ (30). Similar effects of DPQ on NAD^+ and ATP losses after DNA damage have been reported (31). Neither 3-AB nor DPQ (used at >2-fold higher doses than in the above experiments) altered NQO1 activity in enzyme assays *in vitro*. Finally, 3-AB did not affect β-lap-induced ROS formation (data not shown).

To confirm that the energetic consequences of PARP-1 hyperactivation (*e.g.* NAD^+ and ATP losses) were necessary and sufficient for β-lap-induced cell death, the effects of 3-AB or DPQ, on apoptosis, was measured by TUNEL assay. Pretreatment with either inhibitor resulted in a reduction in apoptosis (2% and 15% total apoptosis, respectively for 3-AB and DPQ) compared with 55% in β-lap-treated cells (Fig.

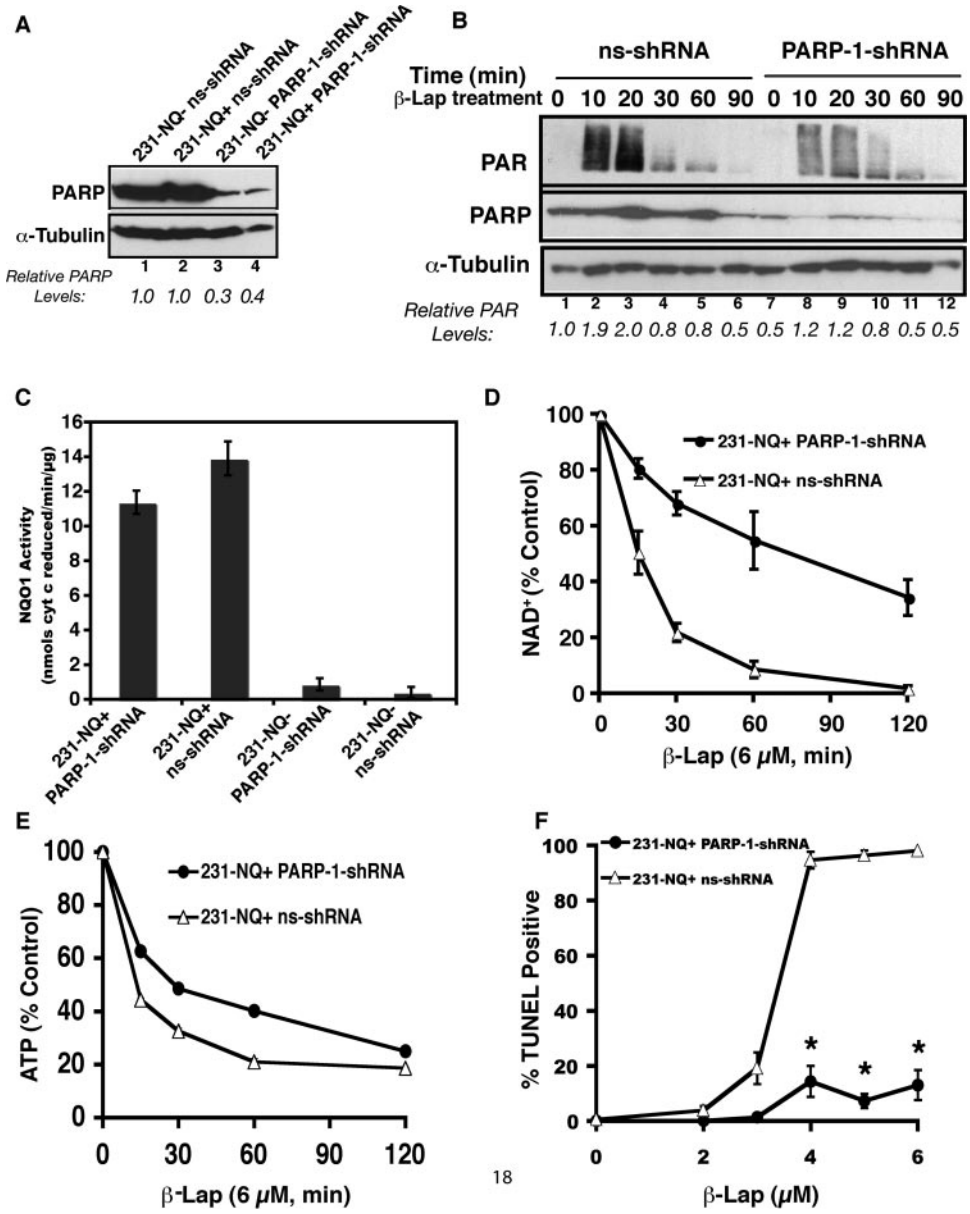

FIGURE 4. **PARP-1 plays an essential role in β-lap-induced apoptotic cell death as monitored by TUNEL.** *A*, immunoblots of steady state PARP-1 and α-tubulin protein levels from whole cell extracts of 231-NQ+ ns-shRNA, 231-NQ+ PARP-1-shRNA, 231-NQ- ns-shRNA, and 231-NQ- PARP-1-shRNA cell lines. Relative PARP-1 protein levels were calculated by densitometry analyses using α-tubulin loading controls by NIH ImageJ wherein controls were set to 1.0. *B*, immunoblots of PAR, PARP-1, and α-tubulin protein levels from control and β-lap (6 μM, 10–90 min)-exposed 231-NQ+ ns-shRNA or PARP-1-shRNA cells. Relative PAR levels were calculated by densitometry analyses using α-tubulin loading controls by NIH ImageJ. *C*, PARP-1 protein knock-down does not alter NQO1 enzymatic activity. NQO1 enzyme activities were determined for 231-NQ+ ns-shRNA, 231-NQ+ PARP-1-shRNA, 231-NQ- ns-shRNA, and 231-NQ- PARP-1-shRNA cells. NQO1 enzyme activities were calculated as nmol of cytochrome *c* reduced/min/μg protein. *D*, PARP-1 is necessary for NAD^+ loss after β-lap exposure. 231-NQ+ ns-shRNA and 231-NQ+ PARP-1-shRNA cells were treated with 6 μM β-lap for 0–120 min at which times NAD^+ content was determined as previously described. *E*, β-lap-induced ATP loss is PARP-1-dependent. ATP levels were monitored in 231-NQ+ ns-shRNA or PARP-1-shRNA cells after exposure to β-lap (6 μM, 0–120 min). Student's *t* test for paired samples, comparing experimental groups 231-NQ+ ns-shRNA *versus* 231-NQ+ PARP-1-shRNA are indicated (*, $p \leq 0.05$; **, $p \leq 0.001$). *F*, knock-down of PARP-1 protein protects cells from β-lap-induced cell death. 231-NQ+ ns-shRNA, and 231-NQ+ PARP-1-shRNA cells were exposed to a 2-h pulse of β-lap and monitored for apoptosis 24-h later. Students's *t* test for paired samples, experimental group compared with vehicle control (*, $p \leq 0.001$).

3*D*). Thus, PARP-1 inhibition by 3-AB or DPQ spared β-lap-induced apoptosis in NQO1+ MCF-7 cells, consistent with the effects of these inhibitors to prevent NAD^+ and ATP losses. Cumulatively, these data strongly suggest that Ca^{2+}-dependent PARP-1 hyperactivation caused NAD^+ and ATP loss in NQO1+ human cancer cell lines after β-lap treatment.

PARP-1 Hyperactivation Is Required for β-lap Cytotoxicity—Because the use of PARP inhibitors was only partially effective at preventing nucleotide loss after β-lap treatment, we confirmed the above findings using a genetic system. NQO1-expressing 231 breast cancer cells were chosen, since they have lower NQO1 levels than MCF-7 cells. PARP-1 protein in 231-NQ+ and 231-NQ− cells was suppressed by stable PARP-1-shRNA expression. Both 231-NQ+ and 231-NQ− cells infected with PARP-1-shRNA showed 3-fold knockdown of PARP-1 protein levels compared with cells containing a non-silencing shRNA sequence (ns-shRNA) (Fig. 4*A*). Poly-(ADP-ribosyl)ation was decreased in 231-NQ+ PARP-1-shRNA cells after β-lap exposure compared with 231-NQ+ ns-shRNA cells (Fig. 4*B*). The remaining PAR-modified proteins noted in cell extracts from β-lap-treated 231-NQ+ PARP-1-shRNA cells were caused by residual PARP-1 activity, since NQO1 activity was not altered after viral knock-down (Fig. 4*C*). PARP-1 protein knock-down spared 231-NQ+ cells from β-lap-induced NAD^+ and ATP losses compared with 231-NQ+ ns-shRNA cells (Fig. 4, *D* and *E*, respectively). Importantly, PARP-1 protein knock-down in 231-NQ+ PARP-1-shRNA cells was sufficient to abrogate β-lap-induced apoptosis at concentrations that killed all 231-NQ+ ns-shRNA cells (Fig. 4*F*). In contrast, without NQO1 activity, nominal PAR accumulation, NAD^+ or ATP losses were observed in 6 μM β-lap-treated 231-NQ- cells containing PARP-1-shRNA or ns-shRNA (data not shown). These cells remained resistant to β-lap independent of altered PARP-1 levels.

NQO1-dependent DNA Damage after β-lap Treatment—To date, there is little direct evidence that β-lap treatment causes DNA damage as assessed by alkaline or neutral filter elution, p53 induction, or covalent complex protein-DNA formation (8, 32, 33). However, many of these prior studies were performed in cells expressing little to no NQO1 (34). PARP-1 hyperactivation typically requires DNA damage,

therefore, we examined NQO1-positive cells exposed to β-lap for DNA breaks, by measuring γ-H2AX. H2AX contains a highly conserved serine residue (Ser^{139}), that is rapidly phosphorylated upon DNA damage (35). Significant γ-H2AX foci formation was observed in 30 min, similar to that seen 15 min following 5 Gy (Fig. 5*A*). In contrast, total H2AX and α-tubulin levels remained unchanged. These results were confirmed by confocal microscopy (Fig. 5*B*).

Because Ca^{2+} chelation blocked both β-lap-induced PARP-1 hyperactivation and cell death, we tested the effects of BAPTA-AM on γ-H2AX foci formation. Similar to the immunoblot analyses and the PAR formation kinetics (Fig. 2*C*), β-lap-treated MCF-7 cells showed γ-H2AX foci in 10 min (~17 foci/cell) of exposure, with peak levels at 60 min (~40 foci/cell) (Fig. 5*C*). Importantly, β-lap-induced γ-H2AX foci formation was partially abrogated by BAPTA-AM addition, with fewer γ-H2AX foci noted in 30–90 min (~5–25 foci/cell respectively) (Fig. 5*C*). These results were confirmed by immunoblot analyses (Fig. 5*D*).

Ca^{2+} Chelation Modulates DNA Repair after β-lap Treatment—We postulated that metabolism of β-lap by NQO1 would generate superoxide, peroxide, and other ROS (36). We directly monitored intracellular ROS formation, using the conversion of non-fluorescent 6-carboxy-2′,7′-dichlorodihydrofluorescin to fluorescent 6-carboxy-2′,7′-dichlorodihydrofluorescein (DCF). Indeed, exposure of MCF-7 cells with 5 or 8 μM β-lap treatment, caused an increase in fluorescence within 5 min compared with Me_2SO-treated cells (Fig. 6*A, left panel*). Region-of-interest analyses showed an ~2000-fold increase in fluorescence with β-lap alone over control cells, which could be abrogated by inhibiting NQO1 activity with dicoumarol (Fig. 6*A*, *right panel*). Because BAPTA-AM has moderate affinity for divalent cations other than Ca^{2+}, we explored the possibility that BAPTA-AM may protect cells from DNA damage and subsequent cell death by interfering with Fenton chemistry. Cells pretreated with 5 μM BAPTA-AM and then exposed to 5 or 8 μM β-lap exhibited no significant difference in the rate or extent of ROS formation compared with β-lap alone-treated cells (Fig. 6*A*). These results were confirmed by examining the oxidative state of MDA-MB-468-NQ+ cells after treatment with 4 μM β-lap in the presence or absence of 5 μM BAPTA-AM. β-lap treatment caused an ~65% rise in disulfide glutathione (GSSG) levels, that persisted during drug exposure (Fig. 6*B*). Addition of BAPTA-AM did not alter the kinetics or levels of GSSG formation during β-lap exposure (Fig. 6*B*). These data suggest that the protective effects of BAPTA-AM on β-lap-treated NQO1+ cells were not caused by interference with β-lap-induced ROS formation. Similar results were found in 231-NQ+ cells (data not shown).

To assess the effects of Ca^{2+} on DNA damage and repair, β-lap-treated MCF-7 cells were analyzed by alkaline comet assays to monitor total DNA strand breaks with or without BAPTA-AM addition. β-lap-treated cells exhibited significant DNA strand breakage by 10 min, resembling the positive control (H_2O_2), and after 30 min, β-lap-induced DNA damage exceeded those levels (Fig. 6*C* and supplemental Fig. S3). Cells pretreated with BAPTA-AM exhibited less DNA damage compared with β-lap alone, and their repair of DNA damage correlated well with their ability (or lack thereof) to survive (Figs. 6*C* and 1*B*).

We then examined the kinetics of repair in MCF-7 cells following a 2-h β-lap exposure with or without BAPTA-AM pretreatment. After β-lap exposure, DNA damage persisted and gradually increased over time (Fig. 6*C*), indicative of inhibition of DNA repair and consistent with the drop in NAD^+ and ATP levels (Fig. 3, *B* and *C*). Although cells treated with β-lap and BAPTA-AM at 2 h exhibited equivalent damage to 10 min of β-lap exposure alone (4.6 ± 0.2 *versus* 4.7 ± 0.4, $p > 0.5$ comet microns, respectively), BAPTA-AM pretreated cells were protected from PARP-1 hyperactivation (Fig. 2*B*), as well as decrements in NAD^+ levels (Fig. 3*B*). BAPTA-AM-pretreated cells showed a time-dependent recovery from DNA damage (Fig. 6*C* and supplemental Fig. S3). In contrast, β-lap-exposed cells showed extensive DNA damage with no signs of DNA repair. Collectively, these data suggest that NQO1-mediated metabolism of β-lap leads to the generation of ROS and subsequent DNA damage that hyperactivates PARP-1.

H_2O_2 Causes Ca^{2+}-dependent PARP-1 Hyperactivation—To examine the universality of Ca^{2+}-modulated PARP-1 function in response to other DNA damaging agents, we examined responses to H_2O_2 or MNNG. Unlike β-lap, H_2O_2 treatment caused PARP-1 hyperactivation in both 231-NQ+ and 231-NQ− cells (Fig. 7*A*). However, expression of NQO1 required higher doses of H_2O_2 to cause PAR formation in 231 cells (Fig. 7*A*). These data suggest that NQO1 has a broader antioxidant role by protecting against ROS-induced damage as previously proposed (37–39). Consistent with β-lap, however, was the abrogation of H_2O_2-induced PAR formation by BAPTA-AM in 231 cells independent of NQO1 activity (Fig. 7*B*).

H_2O_2 treatment also caused a dose-dependent increase in apoptosis in both 231-NQ− and 231-NQ+ cells that was blocked by BAPTA-AM (Fig. 7*C*). However, 231-NQ+ cells were much less sensitive to H_2O_2 than 231-NQ- cells. ATP loss was seen within minutes of H_2O_2 exposure in 231-NQ−, but not in NQO1-positive 231-NQ+ cells (supplemental Fig. S4). In addition, PARP-1 hyperactivation and cell death in response to equivalent doses of H_2O_2 in 231-NQ- cells was much more robust than in 231-NQ+ cells (Fig. 7, *B* and *C*). Interestingly, as noted with β-lap exposure, treatment of MCF-7 cells with ≥200 μM H_2O_2 for 2 h resulted in formation of a 60-kDa PARP-1 and 40-kDa p53 fragments. This atypical proteolysis was effectively inhibited by BAPTA-AM pretreatment (supplemental Fig. S5).

Finally, BAPTA-AM had no effect on PARP-1 hyperactivity or cytotoxicity caused by treatment with the monofunctional DNA-alkylating agent, MNNG (Fig. 7*E*). Because MNNG does not cause Ca^{2+} release like β-lap or H_2O_2, these data suggest that Ca^{2+} modulation of PARP-1 hyperactivation is unique to ROS-producing agents.

DISCUSSION

The regulatory mechanisms controlling PARP-1 function to either promote cell survival or cell death in response to DNA damage remain enigmatic. PARP-1 facilitates DNA repair and cell survival in response to a variety of DNA-damaging agents. However, it also mediates programmed necrosis (17), as well as caspase-inde-

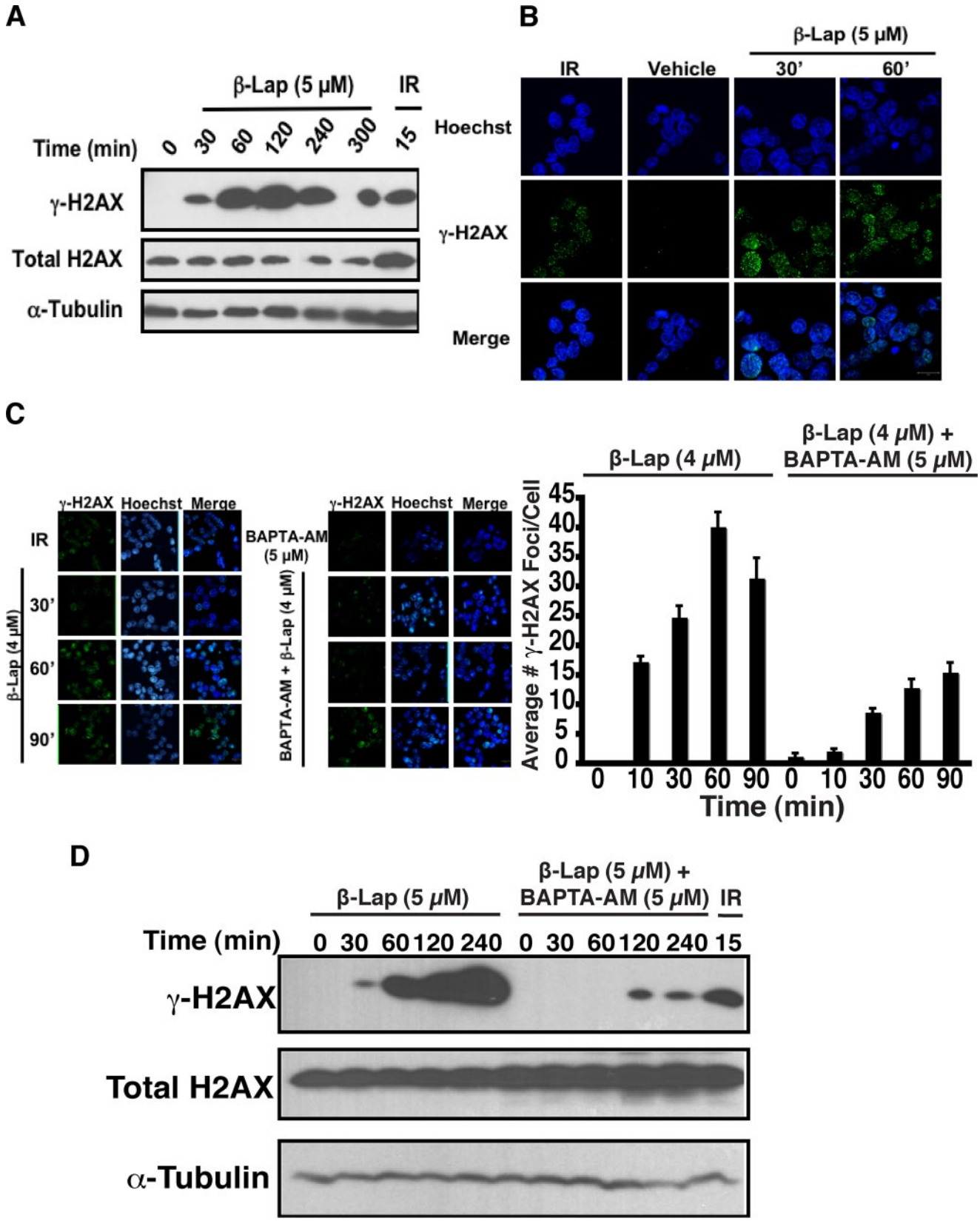

FIGURE 5. **β-lap-induced γ-H2AX foci formation is abrogated by BAPTA-AM pretreatment.** *A*, immunoblot analyses of γ-H2AX, total H2AX, and α-tubulin protein levels in whole cell extracts from MCF-7 cells exposed to β-lap for various times, or IR (5 Gy) harvested after 15 min. *B*, visualization of γ-H2AX foci in MCF-7 cells at various times after treatment with 5 μM β-lap or 15 min post-IR (5 Gy) by confocal microscopy. *C*, BAPTA-AM pretreatment followed by β-lap exposure abrogates γ-H2AX foci formation in MCF-7 cells as visualized by confocal microscopy. The number of γ-H2AX foci per cell was determined from at least 60 cells for each treatment group from four independent confocal experiments (means ± S.E.). *D*, immunoblot of γ-H2AX, total H2AX, and α-tubulin protein levels in whole cell extracts from MCF-7 cells exposed to β-lap for various times with or without BAPTA-AM (5 μM) pretreatment, or IR (5 Gy) harvested after 15 min.

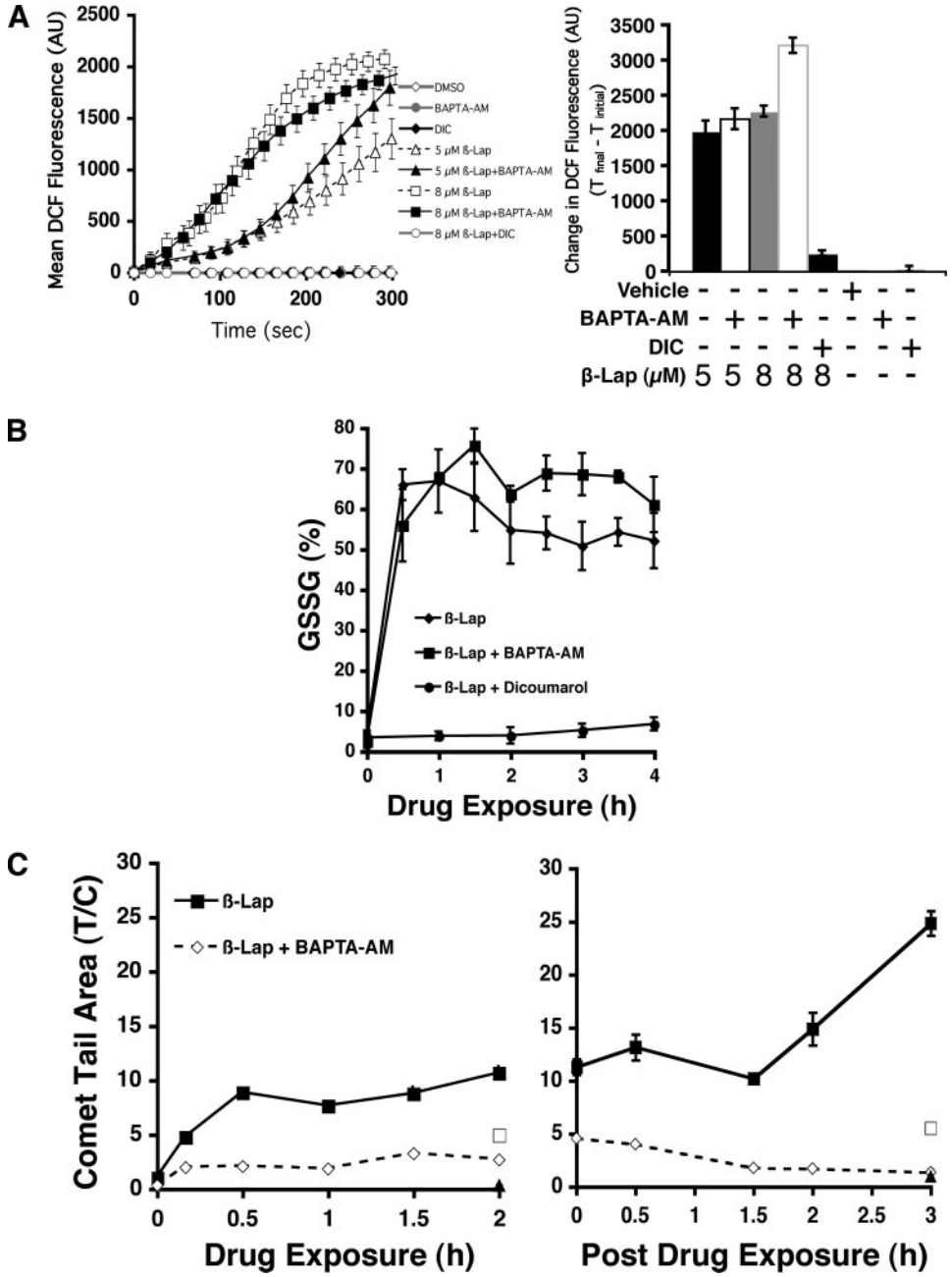

FIGURE 6. **Ca^{2+} modulates DNA repair in β-lap-treated cells.** *A*, β-lap treatment causes the formation of ROS that is not blocked by BAPTA-AM pretreatment. MCF-7 cells were loaded with DCF as described under "Experimental Procedures." Images were collected before drug treatment (0 min) and every 15 s during treatment up to 5 min. Cells were treated with β-lap (5 or 8 μM) with or without BAPTA-AM pretreatment or cotreatment with dicoumoral. Values represent the average of total cellular DCF fluorescence expressed as arbitrary units (AU) from 0–5 min (*left panel*). X-fold changes in fluorescence were calculated as the difference in fluorescence at 5 min minus the initial fluorescence obtained at the time of drug addition (*right panel*). Results are expressed as means ± S.E. from 20–30 cells per treatment group. Shown are representative data from three independent experiments. *B*, BAPTA-AM does not block β-lap-induced ROS production in NQO1+ MDA-MB-468 cells as monitored by changes in levels of disulfide glutathione (%GSSG) following treatment with 4 μM β-lap alone, or in cells pretreated for 30 min with 5 μM BAPTA-AM and then exposed to 4 μM β-lap. *C*, DNA damage in MCF-7 cells during (*left*) or following (*right*) vehicle (Me_2SO) alone, 500 μM H_2O_2 (□), 4 μM β-lap, 5 μM BAPTA-AM (▲) or in MCF-7 cells pretreated with 5 μM BAPTA-AM prior to β-lap (4 μM) exposure. DNA damage was assessed by alkaline comet assays at the indicated times. The comet tail area of 100 cells (means ± S.E.) for each time and condition were quantified with NIH ImageJ software and normalized to untreated cells. Similar results were obtained by analyzing comet tail length.

pendent apoptotic cell death following severe levels of DNA damage (40). The downstream pathways essential for the execution of cell death in response to PARP-1-mediated metabolic alterations remain poorly understood.

In elucidating the cell death pathway after exposure to β-lap, we uncovered a novel mechanism of PARP-1-mediated cell death. Our data suggest that this mechanism occurred selectively in response to ROS-generating agents. We demonstrated, for the first time, that Ca^{2+}-mediated PARP-1 hyperactivation commits cells to death as a consequence of metabolic starvation without the involvement of caspases.

PARP-1 hyperactivation in response to β-lap treatment was not cell type-specific and has been observed in all cells that express elevated NQO1 levels (Fig. 2*A*, and supplemental Fig. S2, *A–C*). As a result, cells exposed to β-lap exhibited depletion of NAD^+ and ATP, occurring 30–60 min during drug exposure. NAD^+ and ATP losses were, in part, PARP-1-mediated since PARP inhibitors (*e.g.* 3-AB and DPQ) partially abrogated nucleotide loss (Fig. 3, *B* and *C*). Chemical inhibition of PARP-1, or PARP-1 protein knock-down, not only prevented NAD^+ and ATP losses, but also abrogated β-lap-induced apoptosis (Figs. 3*D* and 4, *D–F*). These data established PARP-1-mediated NAD^+ and ATP losses as crucial upstream events in β-lap-mediated cell death.

PARP-1-mediated alterations in cellular metabolism caused by β-lap reported in NQO1-expressing cells in this study explain many of its purported effects *in vitro* and *in vivo*. These include, but are not limited to: (i) inhibition of NFκB activation via inhibition of IKK-α (41), (ii) lack of caspase activation (6) and p53 stabilization (8), and (iii) inhibition of Topoisomerase (Topo) I and Topo II-β (42). Furthermore, β-lap can initiate cell death independently from Bax and/or Bak activation as changes in mitochondrial outer membrane permeabilization (MOMP) can occur via PARP-1-mediated NAD^+ loss.[3] Thus, the results reported here appear to explain all prior phenomena reported in cells exposed to β-lap.

[3] W. X., Zong, E. A. Bey, and D. A. Boothman, unpublished data.

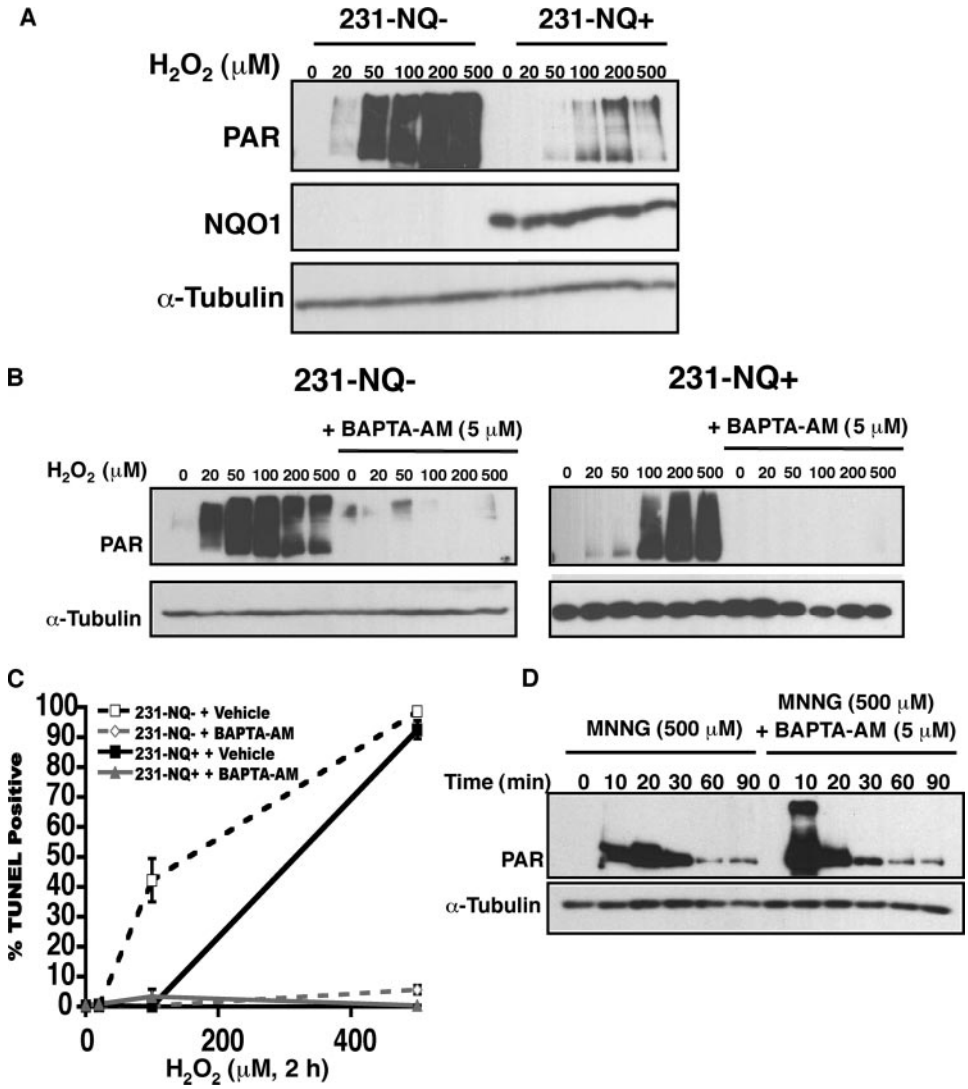

FIGURE 7. **H_2O_2 causes Ca^{2+}-dependent PARP-1 hyperactivation and cell death.** *A*, PARP-1 hyperactivation after H_2O_2 exposure occurs regardless of NQO1 status. Immunoblot analyses of PAR, NQO1, and α-tubulin protein levels in whole cell extracts from 231-NQ- and 231-NQ+ cells after exposure to varying doses of H_2O_2 for 15 min. *B*, PARP-1 hyperactivation after H_2O_2 treatment is Ca^{2+}-dependent. 231-NQ- (*left*) and 231-NQ+ cells (*right*) were pretreated with BAPTA-AM or vehicle alone for 30 min and then treated with varying doses of H_2O_2 and harvested after 15 min. Immunoblots of PAR, and α-tubulin protein levels from whole cell extracts were then analyzed. *C*, Ca^{2+} chelation protects 231-NQ- and 231-NQ+ cells from H_2O_2-induced apoptosis. TUNEL assays were performed in H_2O_2-exposed, log-phase 231-NQ- and 231-NQ+ cells, with or without pretreatment with 5 μM BAPTA-AM. *D*, MNNG-induced PARP-1 hyperactivation is not blocked by Ca^{2+} chelation. Immunoblots of PAR and α-tubulin protein levels from whole cell extracts of MCF-7 cells treated with MNNG or in cells pretreated for 30 min with BAPTA-AM and then exposed to MNNG are shown. Cells were treated for the indicated times and immediately harvested.

A unique feature of PARP-1-mediated cell death stimulated by β-lap was that administration of BAPTA-AM abrogated PARP-1 hyperactivation (Fig. 2*B*, supplemental Fig. S2*D*), nucleotide pool loss (Fig. 3*B*), atypical proteolyses (assessed by p53 and 60 kDa PARP-1 cleavage) (supplemental Fig. S1*B*), and cell death (Fig. 1, *B* and *C*). When BAPTA-AM was added >20 min after β-lap treatment, cells were not protected from cell death (Fig. 1*C*), suggesting that events occurring within the first 20 min of drug exposure committed cells to death. BAPTA (free acid form) did not alter NQO1 activity *in vitro* (24). This appears to be confirmed by the inability of BAPTA-AM to prevent ROS generation, which arises from NQO1-mediated metabolism of β-lap. Instead, our data suggest that the ability of BAPTA-AM to prevent β-lap-induced lethality in NQO1+ cancer cells was caused by the specific prevention of PARP-1 hyperactivation. The observed differences in the amount of DNA damage and γ-H2AX foci formation between β-lap alone and that of β-lap co-administered with BAPTA-AM suggest that preventing PARP-1 hyperactivation and subsequent changes in cellular metabolism can allow for cell recovery, noted by more rapid and extensive DNA damage repair (Figs. 5*C* and 6*C*). Recent data suggest that protein phosphatase 2A (PP2A) dephosphorylates γ-H2AX and is required for DSB repair (43). It is possible that Ca^{2+} chelation not only prevents PARP-1 hyperactivation, but also augments γ-H2AX dephosphorylation through PP2A activity. ROS-induced ER Ca^{2+} release may poison PP2A. However, we favor the theory that NQO1-mediated β-lap-induced ER Ca^{2+} release has its predominant affect on PARP-1 hyperactivation, thereby inhibiting DNA repair and cell recovery.

The mechanism of cell death induced by β-lap could be recapitulated by treatment with high doses of ROS-generating agents, such as H_2O_2 (Fig. 7, *A–D*). Notable similarities included: H_2O_2-mediated PARP-1 hyperactivation, Ca^{2+}-dependent proteolytic cleavage of PARP-1 and p53, and apoptotic DNA fragmentation. Furthermore, H_2O_2-induced lethality was abrogated by BAPTA-AM (Fig. 7, *A–D* and supplemental Fig. S5). Although β-lap and H_2O_2 initiate a similar downstream death pathway, the compounds differed in their lethality in cells with respect to NQO1 expression. β-lap lethality was enhanced in cells that express NQO1, whereas H_2O_2 caused greater cytotoxicity in NQO1-deficient cells (Fig. 7*C*). We noted striking similarities between β-lap- or H_2O_2-induced cell death and the caspase-independent cell death induced by ischemia-reperfusion. ROS produced during ischemia-reperfusion induces DNA strand breaks beyond a normal threshold that lead to PARP-1 hyperactivation, metabolic catastrophe, and an increase in intracellular Ca^{2+} levels leading to μ-calpain activation (44). These data suggest that programmed PARP-1-mediated cell death is a global response to these types of cellular insults.

PARP-1 hyperactivation was also observed following high doses of MNNG, however, this response was not affected by BAPTA-AM (Fig. 7*D*). These data highlight two separate PARP-1 regulatory mechanisms. First, ROS-induced, PARP-1-mediated cell death appears to require Ca^{2+} as a cofactor, whereas alkylation-mediated PARP-1-induced cell death does not. We propose that Ca^{2+} release following ROS-induced stress directly influences PARP-1 and PARG function. Both Mg^{2+} and Ca^{2+} exert significant (≥3-fold increases) allosteric activation of PARP-1 auto(ADP-ribosyl)ation *in vitro* that is inhibited by EDTA addition (45). We, therefore, speculate that Ca^{2+} chelation modulates PAR synthesis by dampening PARP-1 auto(poly-ADP)-ribosylation. Furthermore, since increases in [Ca^{2+}] can inhibit PARG function by up to 50% *in vitro*, maintenance of homeostatic Ca^{2+} levels after drug treatment would, thereby, restore the normal turnover of PAR by PARG, lifting PARP-1 self-inhibition (46). Our data are consistent with the hypothesis that both PAR synthesis and degradation can be modulated by BAPTA-AM to spare the cell from metabolic catastrophe via Ca^{2+}-mediated NAD^+ and ATP losses (Figs. 2*B*, and 3, *B* and *C*) (47). The remaining PARP-1 activity would be necessary for DNA break repair, ultimately providing a survival advantage to damaged cells (Figs. 1*B*, 5*C*, 6*C*, and 7*C*). We are currently exploring the mechanism by which Ca^{2+} modulates PARP-1 hyperactivation and subsequent DNA repair after H_2O_2 or β-lap treatments *versus* MNNG.

There appears to be some disagreement as to the role of Ca^{2+} in PARP-1-dependent cell death. Ca^{2+} can hyperactivate PARP-1 in the absence of DNA breaks (48). In neuronal cells, glutamate caused Ca^{2+}-mediated ROS production through mitochondrial dysfunction, leading to DNA damage, PARP-1 hyperactivation, and cell death. Furthermore, Ca^{2+} chelators, such as BAPTA-AM, EGTA-AM, and Quin-2-AM, protected against other oxidative stress-induced apoptotic and necrotic cell death mechanisms (49, 50). In these studies, Ca^{2+} chelation did not directly inhibit PARP-1 activity, but rather prevented DNA damage by inhibiting ROS. Contrary to these observations, in our system BAPTA-AM did not alter the direct production of ROS or oxidative stress in H_2O_2- or β-lap-exposed cells (Fig. 6*A*). Therefore, there does not appear to be an interference with transition metal-mediated oxidant production by BAPTA-AM (*e.g.* Fenton reaction) as previously suggested after H_2O_2 treatment (51, 52). In fact, our data demonstrate that β-lap caused equivalent ROS production in both β-lap alone and β-lap + BAPTA-AM treated cells. In contrast to β-lap alone-treated cells, cells pretreated with BAPTA-AM did not exhibit notable PARP-1 hyperactivation, associated NAD^+ and ATP losses, and showed a decrease in DNA damage over time (supplemental Table S1). While these data are suggestive of ongoing DNA repair in the presence of Ca^{2+} chelators, we cannot discount that these observations could also be the result of a decrease in the initial amount of DNA damage created in NQO1+ cells in response to β-lap. Initial DNA damage and active DNA repair would be indistinguishable in these experiments. Thus, although we believe it is unlikely, the Ca^{2+}-dependence of PARP-1 hyperactivation could be an indirect consequence of a BAPTA-AM-mediated decrease (*i.e.* protection) in the initial amount of DNA lesions created in response to β-lap. Future studies will address this issue by utilizing DNA repair-compromised NQO1+ cells.

Collectively, our data suggest that PARP-1 is necessary for the initiation of cell death caused by β-lap. To date, however, the endonuclease responsible for the execution of cell death in response to β-lap treatment remains unknown. We therefore propose, that PARP-1-mediated NAD^+ and ATP losses, in addition to PARG-liberated ADP-ribose, causes an influx of Ca^{2+} from extracellular and intracellular sources. Impairment of ATP-dependent membrane/organelle transporters (*e.g.* plasma membrane Ca^{2+} ATPases (PMCA) and sarcoplasmic/endoplasmic reticulum Ca^{2+} ATPases (SERCA)) by ATP loss, and activation of plasma membrane cation channels (*e.g.* transient receptor potential-melastatin-like (TRMP)) by ADP-ribose, leads to high intracellular Ca^{2+} levels (53) sufficient to activate the Ca^{2+}-dependent protease μ-calpain and commit the cell to death. Previous studies from our laboratory have demonstrated that β-lap causes the downstream activation of μ-calpain resulting in its translocation to the nucleus concomitant with nuclear proteolytic cleavage of p53 and PARP-1 (7). Studies from our laboratory indicate that β-lap treatment causes apoptosis-inducing factor (AIF) translocation from the mitochondria to the nucleus, leading to nuclear condensation following μ-calpain activation.[4] To date, the mechanism responsible for PARP-1-mediated AIF release remains unclear. We speculate that AIF release under conditions of DNA damage may be mediated through a concerted effort of both μ-calpain and PARP-1. Disruption of the mitochondrial membrane potential through PARP-1-dependent NAD^+ and ATP losses, in conjunction with μ-calpain-mediated cleavage of Bid or of AIF itself, may mediate its release from the mitochondria (54, 55).

In conclusion, our studies offer new insights into the signal transduction pathways necessary for PARP-1-mediated cell death, providing a connection between PARP-1 hyperactivation and cell death via fluctuations in Ca^{2+} homeostasis. Knowledge of this pathway may be used to understand, and effectively treat, a large number of human pathologies (*e.g.* ischemia-reperfusion during heart attacks and stroke, and diabetes), as well as to enhance current cancer chemotherapeutic agents through modulation of PARP-1 hyperactivation.

Acknowledgments—We thank Drs. John J. Pink (Case Western Reserve University), Craig Thompson (U. of Pennsylvania), Wei-Xing Zong (State University of New York), and Ying Dong (University of Texas Southwestern Medical Center) for helpful discussions.

REFERENCES

1. Green, D. R., and Evan, G. I. (2002) *Cancer Cell* **1,** 19–30
2. Calabrese, C. R., Almassy, R., Barton, S., Batey, M. A., Calvert, A. H., Canan-Koch, S., Durkacz, B. W., Hostomsky, Z., Kumpf, R. A., Kyle, S., Li, J., Maegley, K., Newell, D. R., Notarianni, E., Stratford, I. J., Skalitzky, D., Thomas, H. D., Wang, L. Z., Webber, S. E., Williams, K. J., and Curtin, N. J. (2004) *J. Natl. Cancer Inst.* **96,** 56–67
3. Kim, M. Y., Zhang, T., and Kraus, W. L. (2005) *Genes Dev.* **19,** 1951–1967
4. Jagtap, P., and Szabo, C. (2005) *Nat. Rev. Drug. Discov.* **4,** 421–440

[4] E. A. Bey and D. A. Boothman, unpublished observations.

5. Pink, J. J., Planchon, S. M., Tagliarino, C., Varnes, M. E., Siegel, D., and Boothman, D. A. (2000) *J. Biol. Chem.* **275,** 5416–5424
6. Pink, J. J., Wuerzberger-Davis, S., Tagliarino, C., Planchon, S. M., Yang, X., Froelich, C. J., and Boothman, D. A. (2000) *Exp. Cell Res.* **255,** 144–155
7. Tagliarino, C., Pink, J. J., Reinicke, K. E., Simmers, S. M., Wuerzberger-Davis, S. M., and Boothman, D. A. (2003) *Cancer Biol. Ther.* **2,** 141–152
8. Wuerzberger, S. M., Pink, J. J., Planchon, S. M., Byers, K. L., Bornmann, W. G., and Boothman, D. A. (1998) *Cancer Res.* **58,** 1876–1885
9. Ross, D., Kepa, J. K., Winski, S. L., Beall, H. D., Anwar, A., and Siegel, D. (2000) *Chem. Biol. Interact.* **129,** 77–97
10. Siegel, D., Franklin, W. A., and Ross, D. (1998) *Clin. Cancer Res.* **4,** 2065–2070
11. Nieminen, A. L., Byrne, A. M., Herman, B., and Lemasters, J. J. (1997) *Am. J. Physiol.* **272,** C1286–C1294
12. Dawson, T. L., Gores, G. J., Nieminen, A. L., Herman, B., and Lemasters, J. J. (1993) *Am. J. Physiol.* **264,** C961–C967
13. Olive, P. L., Banath, J. P., and Durand, R. E. (1990) *Radiat. Res.* **122,** 86–94
14. Abramoff, M. D., Magelhaes, P. J., and Ram, S. J. (2004) *Biophotonics Int.* **11,** 36–42
15. Rasband, W. (1997–2005) *Image J. Int.,* Bethesda, MD
16. Jacobson, E. L., and Jacobson, M. K. (1997) *Methods Enzymol.* **280,** 221–230
17. Zong, W. X., Ditsworth, D., Bauer, D. E., Wang, Z. Q., and Thompson, C. B. (2004) *Genes Dev.* **18,** 1272–1282
18. Beigi, R. D., and Dubyak, G. R. (2000) *J. Immunol.* **165,** 7189–7198
19. Fitzsimmons, S. A., Workman, P., Grever, M., Paull, K., Camalier, R., and Lewis, A. D. (1996) *J. Natl. Cancer Inst.* **88,** 259–269
20. Hollander, P. M., and Ernster, L. (1975) *Arch. Biochem. Biophys.* **169,** 560–567
21. Lee, Y. J., Galoforo, S. S., Berns, C. M., Chen, J. C., Davis, B. H., Sim, J. E., Corry, P. M., and Spitz, D. R. (1998) *J. Biol. Chem.* **273,** 5294–5299
22. Blackburn, R. V., Spitz, D. R., Liu, X., Galoforo, S. S., Sim, J. E., Ridnour, L. A., Chen, J. C., Davis, B. H., Corry, P. M., and Lee, Y. J. (1999) *Free Radic. Biol. Med.* **26,** 419–430
23. Lowry, O. H., Rosebrough, N. J., Farr, A. L., and Randall, R. J. (1951) *J. Biol. Chem.* **193,** 265–275
24. Tagliarino, C., Pink, J. J., Dubyak, G. R., Nieminen, A. L., and Boothman, D. A. (2001) *J. Biol. Chem.* **276,** 19150–19159
25. Jacobsen, M. D., Weil, M., and Raff, M. C. (1996) *J. Cell Biol.* **133,** 1041–1051
26. D'Amours, D., Desnoyers, S., D'Silva, I., and Poirier, G. G. (1999) *Biochem. J.* **342,** 249–268
27. Szabo, C., and Dawson, V. L. (1998) *Trends Pharmacol. Sci.* **19,** 287–298
28. Pieper, A. A., Verma, A., Zhang, J., and Snyder, S. H. (1999) *Trends Pharmacol. Sci.* **20,** 171–181
29. McLick, J., Hakam, A., Bauer, P. I., Kun, E., Zacharias, D. E., and Glusker, J. P. (1987) *Biochim. Biophys. Acta* **909,** 71–83
30. Southan, G. J., and Szabo, C. (2003) *Curr. Med. Chem.* **10,** 321–340
31. Cipriani, G., Rapizzi, E., Vannacci, A., Rizzuto, R., Moroni, F., and Chiarugi, A. (2005) *J. Biol. Chem.* **280,** 17227–17234
32. Boothman, D. A., and Pardee, A. B. (1989) *Proc. Natl. Acad. Sci. U. S. A.* **86,** 4963–4967
33. Boothman, D. A., Wang, M., Schea, R. A., Burrows, H. L., Strickfaden, S., and Owens, J. K. (1992) *Int. J. Radiat. Oncol. Biol. Phys.* **24,** 939–948
34. Boothman, D. A., Meyers, M., Fukunaga, N., and Lee, S. W. (1993) *Proc. Natl. Acad. Sci. U. S. A.* **90,** 7200–7204
35. Rogakou, E. P., Pilch, D. R., Orr, A. H., Ivanova, V. S., and Bonner, W. M. (1998) *J. Biol. Chem.* **273,** 5858–5868
36. Reinicke, K. E., Bey, E. A., Bentle, M. S., Pink, J. J., Ingalls, S. T., Hoppel, C. L., Misico, R. I., Arzac, G. M., Burton, G., Bornmann, W. G., Sutton, D., Gao, J., and Boothman, D. A. (2005) *Clin. Cancer Res.* **11,** 3055–3064
37. Siegel, D., Gustafson, D. L., Dehn, D. L., Han, J. Y., Boonchoong, P., Berliner, L. J., and Ross, D. (2004) *Mol. Pharmacol.* **65,** 1238–1247
38. Lewis, A., Ough, M., Li, L., Hinkhouse, M. M., Ritchie, J. M., Spitz, D. R., and Cullen, J. J. (2004) *Clin. Cancer Res.* **10,** 4550–4558
39. Cullen, J. J., Hinkhouse, M. M., Grady, M., Gaut, A. W., Liu, J., Zhang, Y. P., Weydert, C. J., Domann, F. E., and Oberley, L. W. (2003) *Cancer Res.* **63,** 5513–5520
40. Yu, S. W., Wang, H., Poitras, M. F., Coombs, C., Bowers, W. J., Federoff, H. J., Poirier, G. G., Dawson, T. M., and Dawson, V. L. (2002) *Science* **297,** 259–263
41. Manna, S. K., Gad, Y. P., Mukhopadhyay, A., and Aggarwal, B. B. (1999) *Biochem. Pharmacol.* **57,** 763–774
42. Pardee, A. B., Li, Y. Z., and Li, C. J. (2002) *Curr. Cancer Drug. Targets* **2,** 227–242
43. Chowdhury, D., Keogh, M. C., Ishii, H., Peterson, C. L., Buratowski, S., and Lieberman, J. (2005) *Mol. Cell* **20,** 801–809
44. van Wijk, S. J., and Hageman, G. J. (2005) *Free Radic Biol. Med.* **39,** 81–90
45. Kun, E., Kirsten, E., Mendeleyev, J., and Ordahl, C. P. (2004) *Biochemistry* **43,** 210–216
46. Tanuma, S., Kawashima, K., and Endo, H. (1986) *J. Biol. Chem.* **261,** 965–969
47. Ogata, N., Ueda, K., Kawaichi, M., and Hayaishi, O. (1981) *J. Biol. Chem.* **256,** 4135–4137
48. Homburg, S., Visochek, L., Moran, N., Dantzer, F., Priel, E., Asculai, E., Schwartz, D., Rotter, V., Dekel, N., and Cohen-Armon, M. (2000) *J. Cell Biol.* **150,** 293–307
49. Virag, L., Scott, G. S., Antal-Szalmas, P., O'Connor, M., Ohshima, H., and Szabo, C. (1999) *Mol. Pharmacol.* **56,** 824–833
50. Barbouti, A., Doulias, P. T., Zhu, B. Z., Frei, B., and Galaris, D. (2001) *Free Radic Biol. Med.* **31,** 490–498
51. Jornot, L., Petersen, H., and Junod, A. F. (1998) *Biochem. J.* **335,** 85–94
52. Britigan, B. E., Rasmussen, G. T., and Cox, C. D. (1998) *Biochem. Pharmacol.* **55,** 287–295
53. Fonfria, E., Marshall, I. C., Benham, C. D., Boyfield, I., Brown, J. D., Hill, K., Hughes, J. P., Skaper, S. D., and McNulty, S. (2004) *Br. J. Pharmacol.* **143,** 186–192
54. Polster, B. M., Basanez, G., Etxebarria, A., Hardwick, J. M., and Nicholls, D. G. (2005) *J. Biol. Chem.* **280,** 6447–6454
55. Takano, J., Tomioka, M., Tsubuki, S., Higuchi, M., Iwata, N., Itohara, S., Maki, M., and Saido, T. C. (2005) *J. Biol. Chem.* **280,** 16175–16184

Nonhomologous End Joining Is Essential for Cellular Resistance to the Novel Antitumor Agent, β-Lapachone

Melissa S. Bentle,[1] Kathryn E. Reinicke,[2] Ying Dong,[3] Erik A. Bey,[3] and David A. Boothman[3]

Departments of [1]Pharmacology and [2]Biochemistry, Case Western Reserve University, Cleveland, Ohio; and [3]Department of Pharmacology, Laboratory of Molecular Stress Responses, and the Simmons Comprehensive Cancer Center, University of Texas Southwestern Medical Center, Dallas, Texas

Abstract

Commonly used antitumor agents, such as DNA topoisomerase I/II poisons, kill cancer cells by creating nonrepairable DNA double-strand breaks (DSBs). To repair DSBs, error-free homologous recombination (HR), and/or error-prone nonhomologous end joining (NHEJ) are activated. These processes involve the phosphatidylinositol 3′-kinase–related kinase family of serine/threonine enzymes: *ataxia telangiectasia* mutated (ATM), ATM- and Rad3-related for HR, and DNA-dependent protein kinase catalytic subunit (DNA-PKcs) for NHEJ. Alterations in these repair processes can cause drug/radiation resistance and increased genomic instability. β-Lapachone (β-lap; also known as ARQ 501), currently in phase II clinical trials for the treatment of pancreatic cancer, causes a novel caspase- and p53-independent cell death in cancer cells overexpressing NAD(P)H:quinone oxidoreductase-1 (NQO1). NQO1 catalyzes a futile oxidoreduction of β-lap leading to reactive oxygen species generation, DNA breaks, γ-H2AX foci formation, and hyperactivation of poly(ADP-ribose) polymerase-1, which is required for cell death. Here, we report that β-lap exposure results in NQO1-dependent activation of the MRE11-Rad50-Nbs-1 complex. In addition, ATM serine 1981, DNA-PKcs threonine 2609, and Chk1 serine 345 phosphorylation were noted; indicative of simultaneous HR and NHEJ activation. However, inhibition of NHEJ, but not HR, by genetic or chemical means potentiated β-lap lethality. These studies give insight into the mechanism by which β-lap radiosensitizes cancer cells and suggest that NHEJ is a potent target for enhancing the therapeutic efficacy of β-lap alone or in combination with other agents in cancer cells that express elevated NQO1 levels. [Cancer Res 2007;67(14):6936–45]

Introduction

Many cancer chemotherapeutic agents, such as ionizing radiation (IR), and DNA-damaging chemotherapeutic compounds cause cell death by creating DNA double-strand breaks (DSBs; refs. 1, 2). DSBs can occur from endogenously produced reactive oxygen species (ROS) or conversion of single-strand breaks (SSBs) to DSBs by advancing replication forks (3). Although cells maintain the capability to survive low levels of DNA damage, as little as one nonrepaired DSB can be lethal (4).

Homologous recombination (HR) and nonhomologous end joining (NHEJ) are two distinct, yet complementary, mechanisms for mammalian DSB repair that can interact simultaneously at DSB sites (5–7). Essential to both HR and NHEJ is the activation of one or all three related phosphatidylinositol 3′-kinase–like kinases (PI3K) in response to DNA damage (7). *Ataxia telangiectasia* mutated (ATM) and ATM- and Rad3-related (ATR) are associated with HR and are typically activated during S-G_2 phase by DNA breaks (e.g., ATM) or after replication fork arrest (e.g., ATR activation). In contrast, DNA-protein kinase catalytic subunit (DNA-PKcs; part of the DNA-PK complex including the Ku70/Ku80 heterodimer) is involved in NHEJ that operates throughout the cell cycle in response to DSBs. These kinases operate as transducer proteins, relaying and amplifying damage signals to mediator proteins. A common substrate of all PI3Ks is the histone variant, H2AX. Formation of phosphorylated H2AX (γ-H2AX) is a sensitive and early marker of DSBs (8, 9). Shortly after DSB detection and PI3K activation, H2AX becomes phosphorylated on serine 139 (γ-H2AX) in a 2-Mb region surrounding the break. Microscopically, this phosphorylation event occurs on a multitude of H2AX molecules leading to foci that are visible when labeled with an antibody specific for γ-H2AX. γ-H2AX foci facilitate the recruitment of DNA damage–regulating protein complexes to the sites of damage (10), whereas γ-H2AX dephosphorylation assists repair (11). The MRE11/Rad50/Nbs-1 (MRN) complex serves as the initial protein complex to participate in both NHEJ and HR repair pathways (12). In NHEJ, the MRN complex modifies DSB ends by its endonuclease and exonuclease activity (13). In HR, the complex acts as an exonuclease to produce 3′ single-strand overhangs bound by Rad52 (12).

β-Lapachone (β-lap; also known as ARQ 501) is currently in phase II clinical trials for the treatment of pancreatic adenocarcinoma in combination with gemcitabine.[4] β-Lap is a novel antitumor agent that is bioactivated by the two-electron oxidoreductase, NAD(P)H quinone oxidoreductase-1 (NQO1; EC 1.6.99.2). Because NQO1 is highly expressed in many human cancers (e.g., pancreatic, breast, lung, and prostate cancers), it is an attractive target for selective cancer chemotherapy by β-lap alone or with IR (14–16). β-Lap–induced cell death is triggered by the NQO1-dependent oxidoreduction of β-lap (14), resulting in a futile cycling wherein β-lap is reduced to an unstable hydroquinone that spontaneously reverts to its parent structure using two oxygen molecules (17). As a result, ROS are generated causing DNA damage, γ-H2AX foci formation, poly(ADP-ribose) polymerase-1 (PARP-1) hyperactivation, and subsequent loss of ATP and NAD^+ (18). β-Lap–induced cell

Note: Supplementary data for this article are available at Cancer Research Online (http://cancerres.aacrjournals.org/).

Requests for reprints: David A. Boothman, Departments of Pharmacology, Oncology and Radiation Oncology, Laboratory of Molecular Stress Responses Program in Cell Stress and Nanomedicine, and the Simmons Comprehensive Cancer Center, University of Texas Southwestern Medical Center, ND2.210K 5323 Harry Hines Boulevard, Dallas, TX 75390. Phone: 214-645-6371; Fax: 214-645-6437; E-mail: David.Boothman@UTSouthwestern.edu.

doi:10.1158/0008-5472.CAN-07-0935

[4] http://clinicaltrials.gov/ct/show/NCT00102700?order=4 and http://clinicaltrials.gov/ct/show/NCT00358930?order=5

death was unique in that PARP-1 and p53 proteolysis occurred concomitant with μ-calpain activation (17). β-Lap–mediated cell death exhibited classic features of apoptosis (e.g., DNA condensation and terminal deoxynucleotidyl transferase-mediated dUTP nick-end labeling–positive cells), but was not dependent on typical apoptotic mediators, such as p53, Bax/Bak, or caspases (19).

To date, few studies explored the contribution of DSB repair in β-lap–induced cell death. We showed that β-lap caused DNA damage, γ-H2AX focus formation and PARP-1 hyperactivation selectively in NQO1-expressing ($NQO1^+$) cells (18). We therefore investigated whether β-lap exposure of $NQO1^+$ cancer cells activated HR and/or NHEJ, and explored the extent to which these repair systems influenced cellular sensitivity. Various model cell systems with altered ATM, ATR, or DNA-PKcs functions, as well as use of selective kinase inhibitors were used. β-Lap caused a delayed (10–15 min) dose-dependent activation of the MRN complex, as well as ATM, DNA-PKcs, and ATR compared with IR. Importantly, only inhibition of DNA-PKcs enhanced β-lap potency, indicating a predominant role for NHEJ in DSB repair, and resistance of cancer cells to this agent. These results suggest the combinatorial use of NHEJ inhibitors to enhance β-lap cytotoxicity for the treatment of human cancers that express elevated NQO1 levels.

Materials and Methods

Reagents. β-Lap was synthesized by Dr. William G. Bornmann (M.D. Anderson Cancer Center, Houston, TX), dissolved in DMSO at 40 mmol/L, and the concentration was verified by spectrophotometry (18). Hoechst 33258, etoposide, and dicoumarol were obtained from Sigma (St. Louis, MO). The DNA-PKcs inhibitor, Nu7026 (2-(morpholin-4-yl)-benzo[*h*]chromen-4-one), and ATM/ATR kinase inhibitor (AAI) were obtained from Calbiochem. They were dissolved in DMSO and used at 10 μmol/L unless otherwise stated. 2-Morpholin-4-yl-6-thianthren-1-yl-pyran-4-one (KU-55933) was synthesized by KuDOS Pharmaceuticals Ltd., dissolved in DMSO, and used at 10 μmol/L.

Cell culture. MCF-7 breast cancer cells were maintained and used as described (14). Human MO59K and MO59J cells, proficient and deficient in both DNA-PK activity and p350 protein, respectively (20), were obtained from Dr. Joan Turner (University of Alberta). U2OS-derived stable cell lines that conditionally regulate wild-type (WT) or kinase-dead ATR (KD-ATR) levels by doxycycline were generously provided by Drs. Paul Nghiem and Stuart L. Schreiber (Harvard University, Cambridge, MA; ref. 21). Recombinant ATM was stably expressed in immortalized human A-T cells using an episomal expression vector (22) and designated: A-T cells ($ATM^{-/-}$) and A-T cells ectopically expressing ATM ($ATM^{+/+}$). MO59K, MO59J, $ATM^{-/-}$, and $ATM^{+/+}$ cells were stably infected using a puromycin-selectable pLPCX retroviral vector alone or one containing the NQO1 cDNA packaged in Phoenix-Ampho cells (23). Uninfected cells were removed by puromycin selection (0.5 μg/mL). However, all experiments were done without selection. NQO1 expression was evaluated in all cells as described (14). All cells were grown in high glucose-containing DMEM containing 10% fetal bovine serum (FBS) or tetracycline-free FBS (U2OS cells), 2 mmol/L L-glutamine, penicillin (100 units/mL), and streptomycin (100 mg/mL) at 37°C in a 5% CO_2, 95% air humidified atmosphere (24). All tissue culture components were purchased from Invitrogen. Cells were free of *Mycoplasma* contamination.

Relative survival assays. Relative survival assays were done as described (14). MCF-7, MO59K, and MO59J cells were pretreated for 1 h with 10 μmol/L Nu7026 or KU-55933 before cotreatment with β-lap at the indicated doses for 2 to 4 h. After β-lap treatment, medium containing Nu7026 or KU-55933 alone was added and then removed after 16 h. Drug-free medium was added and survival was assessed after 6 days. U2OS WT or KD-ATR cells were treated with 1 μg/mL doxycycline 48 h before treatment with various β-lap doses, with or without dicoumarol (40 μmol/L) for 2 to 4 h, then replaced with drug-free medium. Prior studies using β-lap showed that relative survival assays correlated directly with colony-forming ability (14). Data were expressed as means ±SE for treated versus control from separate triplicate experiments, and comparisons were analyzed using a two-tailed Student's *t* test for paired samples.

Cell irradiation. For UV light C (UVC) exposures, U2OS WT and KD-ATR culture medium were removed, and then placed uncovered under a UV lamp emitting primarily 254 nm radiation (fluency rate of 2.2 $J/m^2/s$). After exposure, medium was replaced and cultures incubated for various times. Other cells were treated with 10 μmol/L β-lap or 500 μmol/L H_2O_2 and harvested for immunoblotting 2 h after treatment. For IR, cells were irradiated using a ^{137}Cs source as described and analyzed for foci formation (see below; ref. 25).

Immunoblotting. Western blots were prepared as described (19) with modifications. To examine Chk1, whole-cell extracts were prepared using lysis buffer [50 mmol/L Tris (pH 8.0), 150 mmol/L NaCl, 1 mmol/L EDTA, 1 mmol/L EGTA, 1% NP40, 10 μL/mL protease inhibitor mixture, and 1 mmol/L sodium metavanadate]. Total α-Chk-1 and the α-phospho-Ser345 Chk-1 (Chk1-pSer345) antibody were used at a dilution of 1:100 (Cell Signaling Technology) and α-tubulin was used at a dilution of 1:5,000 (Calbiochem). An NQO1 antibody was generously provided to us by Dr. David Ross (University of Colorado Health Science Center, Denver, CO) and used at a 1:2,000 dilution (26).

Confocal microscopy. MCF-7 cells were treated with 1 to 5 μmol/L β-lap for various times with or without pretreatment and cotreatment with Nu7026, KU-55933, or DMSO. As a positive control for DSB damage responses, cells were irradiated with 5 Gy and fixed 15 min later. After treatment, cells were fixed in methanol/acetone (1:1) and incubated with primary antibodies: α-MRE11, α-Rad50 (GeneTex), α-Nbs-1 phospho-Ser343 (Nbs-1-p; Abcam), α-ATM phospho-Ser1981, α-DNA-PKcs phospho-Thr2609 (Rockland), or α-γ-H2AX (Trevigen; Upstate) overnight at 4°C at 1:100 to 500 dilutions. Alexa Fluor fluorescent secondary antibodies (Molecular Probes) were added for 2 h at room temperature. Nuclei were visualized by Hoechst 33258 staining at 1:3,000 dilution. Confocal images were collected using a ×63 numerical aperture 1.4 oil immersion planapochromat objective at 488 and 594 nm from argon/HeNe1 lasers, respectively, using a Zeiss LSM 510 confocal microscope. All Hoescht 33258-stained nuclear images were collected using a Coherent Mira-F-V5-XW-220 Ti-Sapphire laser tuned at 750 nm. Images shown were representative of experiments done at least thrice. The average number of foci/μ slice was calculated as means ±SE by counting ≥30 cells from three independent experiments. Student's *t* tests were used for comparison.

Alkaline and neutral comet assays. Single-cell gel electrophoretic comet assays were done under alkaline or neutral conditions (18). MCF-7 cells were treated with 5 μmol/L β-lap, 100 μmol/L etoposide, 500 μmol/L H_2O_2, or vehicle alone and harvested at various times. For neutral comet assays, after cellular lysis, slides were immersed in neutral buffer [1 × Tris-borate EDTA (pH 7.0)] for 60 min at room temperature in the dark. Each data point represents the average of 100 cells ±SE, and data are representative of experiments done in duplicate.

Results

MRN complex activation by β-lap. Previously, we showed that exposure of NQO1-expressing cancer cells to β-lap caused ROS and DNA damage, measured by alkaline comet assays and γ-H2AX formation (18). Furthermore, activation of the MRN complex following β-lap exposure was recently reported in *Saccharomyces cerevisiae* (27). We wanted to determine if, and which, DSB repair pathways were activated in response to β-lap by examining MRN complex recruitment. Although the true nature of damage-induced foci has not been elucidated, these protein complexes are suggested to be a visual indication of DNA repair centers (10). Because the MRN complex is central to both

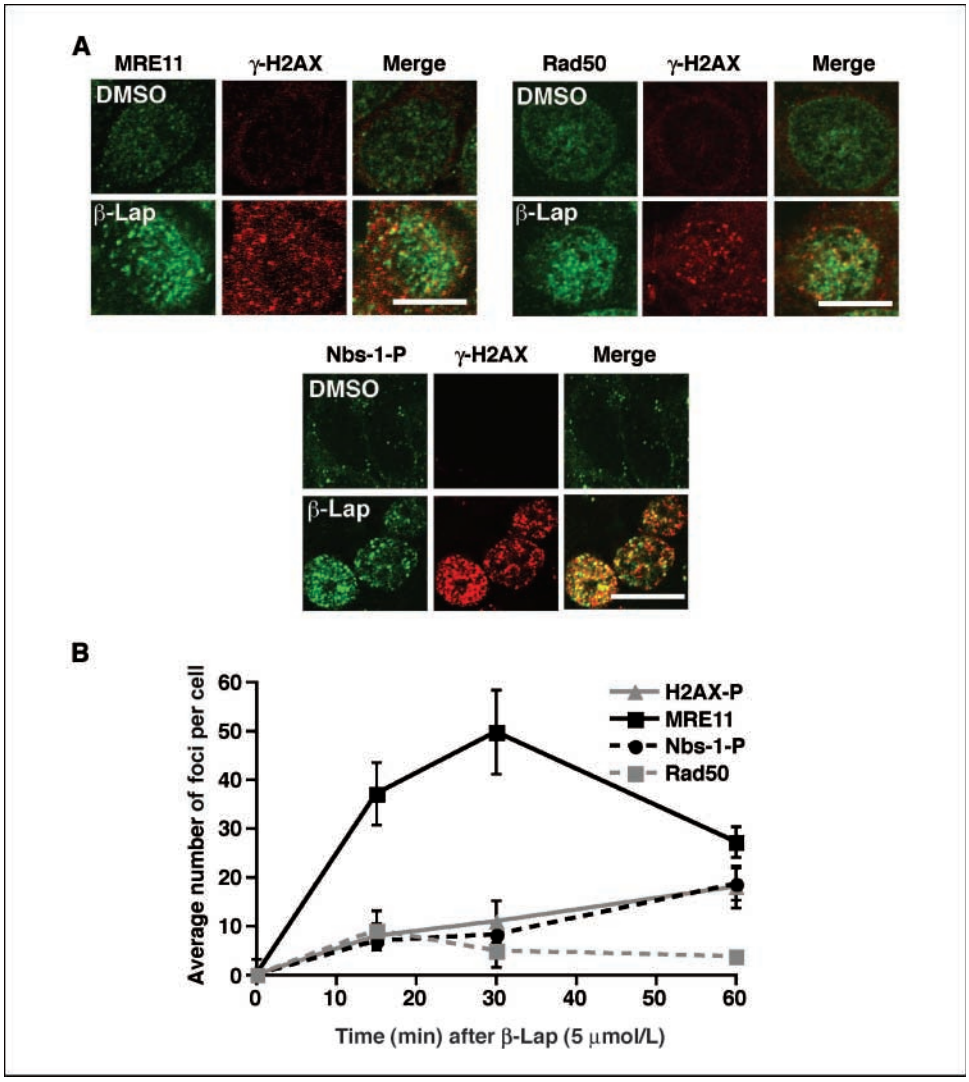

Figure 1. The MRN complex is activated upon β-lap treatment. β-Lap causes punctate nuclear localization of MRE11, Rad50, and phosphorylation of Nbs-1. *A,* visualization of MRE11, Rad50, Nbs-1-p, and γ-H2AX in MCF-7 cells at various times after treatment for 30 min with 5 μmol/L β-lap by confocal microscopy. *B,* average number of MRE11, Rad50, Nbs-1-p, and γ-H2AX foci per cell was determined from ≥60 cells for each treatment group from three independent confocal experiments. *Points,* means; *bars,* SE. Bar, 20 μm.

HR and NHEJ, we examined foci formation in MCF-7 cells after various times of β-lap exposure. Mock- or β-lap–treated cells were stained with antibodies complementary to MRE-11, Rad50, and phosphorylated Ser343 Nbs-1 (Nbs-1-p). Increases in the organized localization of MRE-11 and Rad50 were observed in the nuclei of β-lap–treated cells at 15 min and foci persisted >60 min (Fig. 1*A* and *B*). Similarly, Nbs-1-p nuclear foci were visible beginning 15 min after drug exposure, with similar kinetics as γ-H2AX (Fig. 1*A* and *B*); both proteins are downstream targets of ATM activation (28). MRN complex foci were not visible prior to 15 min β-lap exposure (data not shown). Foci formation was delayed compared with foci observed after IR exposure, in which prior studies have shown γ-H2AX foci formation within 1 to 5 min post-IR (29). Interestingly, with IR-treated cells MRN foci randomly appeared throughout the nucleus, whereas with β-lap–treated cells all components of the MRN formed foci that were predominantly perinuclear (Fig. 1*A*; Supplementary Fig. S1*A*–*C*). The appearance of perinuclear MRN foci is consistent with the fact that NQO1 is largely cytoplasmic (30) and where ROS would diffuse into the nucleus, leading to SSBs. SSBs may then be converted to DSBs at a later time, thereby explaining the delayed activation of the MRN complex.

Dose-dependent activation of ATM and DNA-PK after β-lap treatment. Because the MRN complex was recruited after exposure to β-lap, we examined cells for activation of ATM, a HR-associated PI3K. After interacting with a DSB, ATM undergoes autophosphorylation at serine 1981, causing dissociation of the ATM homodimer (31). Activated ATM monomers phosphorylate numerous downstream proteins, including Nbs-1 (28). To test for ATM activation, MCF-7 cells were mock-treated or exposed to various β-lap doses. Fixed cells were stained with a serine 1981 phosphospecific antibody to ATM (ATM-pSer1981). ATM activation occurred in a dose-dependent manner after β-lap treatment. β-Lap doses (0–3 μmol/L) resulted in few activated ATM molecules, consistent with low levels of DNA damage detected at these doses (Supplementary Fig. S2*A*; Fig. 2*A*). In contrast, lethal doses of β-lap (≥4 μmol/L) caused considerable ATM activation with an ~8-fold increase in the number of foci per cell, corresponding to the net increase in total damage (Supplementary Fig. S2*A*; Fig. 2*A* and *C*). These data suggest that the accumulation of large numbers of β-lap–induced SSBs lead to DSBs that, in turn, activate the canonical HR DSB repair pathway involving MRN and ATM.

Due to the cell cycle independence of NQO1-mediated bioactivation of β-lap (24) and generation of DNA damage, we

examined DNA-PK activation, as it functions in a cell cycle–independent manner (19). Prior work indicated that DNA-PKcs was autophosphorylated at Thr2609 (DNA-PKcs-pThr2609) *in vivo* in response to IR, and DNA-PKcs-pThr2609 colocalizes with γ-H2AX after damage (32, 33). MCF-7 cells were mock-treated or exposed to 1 to 5 μmol/L β-lap for 30 min. Similar to ATM activation, DNA-PKcs-pThr2609 foci formed in a dose-dependent manner. Nontoxic β-lap doses caused few (≥2 foci/cell) DNA-PKcs-pThr2609 foci over background, whereas lethal doses led to increases in DNA-PKcs-pThr2609 foci that colocalized with γ-H2AX (ref. 32; Fig. 2*B*; Supplementary Fig. S2*B*). Importantly, at 3 μmol/L β-lap (~LD_{50} for MCF-7 cells), DNA-PKcs was significantly activated (9 ± 0.2 foci per cell) whereas ATM and γ-H2AX were not as robustly activated (3.9 foci per cell ±1.98 and 3.0 foci per cell ±0.12, respectively). These data suggest that both HR and NHEJ are activated after β-lap exposure, but the predominant DNA repair pathway activated is NHEJ (Fig. 2*C*).

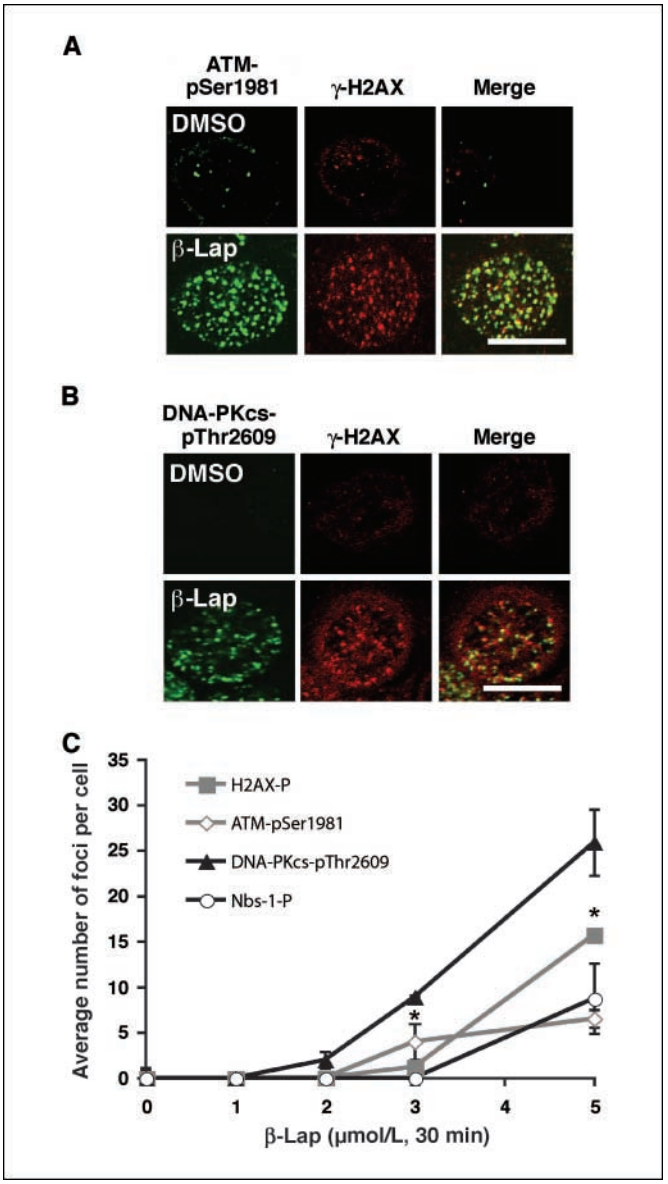

Figure 2. Dose-dependent ATM and DNA-PK activation after β-lap administration. MCF-7 cells were treated with 0 to 5 μmol/L β-lap for 30 min at which time samples were fixed and probed with antibodies to phosphorylated ATM at Ser1981 (*ATM-pSer1981*; *A*) or phosphorylated DNA-PKcs at Thr2609 (*DNA-Pkcs-pThr2609*; *B*) and visualized by confocal microscopy. *C,* MCF-7 cells were treated with 0 to 5 μmol/L β-lap for 30 min; fixed; and probed for ATM-pSer1981, DNA-PKcs-pThr2609, and Nbs-1-p after 30 min. Quantitation of the average number of foci per cell per dose of β-lap–treated cells for ≥60 cells per treatment. *Points,* means; *bars,* SE. Student's *t* test for paired samples, comparing Nbs-1-p or γ-H2AX foci per cell versus the number of DNA-PKcs-pThr2609 foci per cell at various doses of β-lap (*, $P < 0.05$). Bar, 20 μm.

NHEJ is necessary for β-lap–induced cell death. Due to the robust DNA-PK activation after β-lap exposure, we examined the consequences of its inhibition on lethality. Glioblastoma cell lines, MO59K, containing DNA-PKcs and MO59J cells lacking DNA-PKcs, were used (34). These cells lacked NQO1 and were resistant to β-lap. After isolating NQO1-expressing pooled variants, MO59K (MO59K-NQ^+) and MO59J (MO59J-NQ^+) cells had NQO1 enzymatic activities of 790 ± 20 and 690 ± 10 μmol/cytochrome *c* reduced/μg protein, respectively. MO59J-NQ^+ and MO59K-NQ^+ were mock treated or exposed to various β-lap doses for 2 h, with or without dicoumarol cotreatment (a selective NQO1 inhibitor). DNA-PKcs–deficient MO59J-NQ^+ cells were significantly more sensitive to β-lap than their DNA-PKcs–proficient counterparts, MO59K-NQ^+ cells (Fig. 3*A*). MO59J-NQ^+ cells required doses of ~5 μmol/L β-lap to elicit cell death, whereas MO59K-NQ^+ cells were resistant, with only 30% cytotoxicity by 12 μmol/L β-lap. In both cell lines, cytotoxicity was abrogated by inhibiting NQO1 activity with 40 μmol/L dicoumarol (Fig. 3*A*). To assess DNA-PKcs functionality, we pretreated both MO59J-NQ^+ and MO59K-NQ^+ cells with a DNA-PKcs selective inhibitor Nu7026 before β-lap exposure. Nu7026 is a potent radiosensitizer in both proliferating and quiescent cells (35). As anticipated, Nu7026 had little effect on β-lap–induced cell death in MO59J-NQ^+ cells because they are devoid of DNA-PKcs activity. In contrast, Nu7026 significantly sensitized MO59K-NQ^+ cells to β-lap (Fig. 3*B*). Treatment with Nu7026 and 12 μmol/L β-lap resulted in an ~80 ± 3% reduction in survival versus ~5 ± 1% loss of survival in MO59K-NQ^+ cells that were pretreated with vehicle (Fig. 3*B*).

To confirm that DNA-PK was essential in resistance to β-lap–induced cell death, MCF-7 cells were treated with sublethal doses of β-lap with or without pretreatment and cotreatment with 30 μmol/L Nu7026 for 2 h and relative survival was determined. β-Lap doses ≤2 μmol/L had little to no cytotoxicity alone, whereas β-lap doses 2.5 μmol/L and higher caused significant lethality. When MCF-7 cells were treated with Nu7026 and β-lap, lethality was potentiated (Fig. 3*C*). Significant differences in cell death were noted at 2 to 2.5 μmol/L β-lap, where cotreatment with otherwise nontoxic doses of Nu7026 and β-lap resulted in a >80% reduction in survival compared with cells treated with β-lap alone (Fig. 3*C*). To confirm that DNA-PKcs and not ATM was important in β-lap–induced cell death, MCF-7 cells were treated with 5 μmol/L β-lap alone with or without pretreatment and cotreatment with 30 μmol/L Nu7026. Effects on DNA-PKcs versus ATM foci formation were then assessed. After 30 min of β-lap exposure, cells were fixed and stained with antibodies to both DNA-PKcs-pThr2609 and ATM-pSer1981 and the average number of foci per cell were examined by confocal microscopy. β-Lap–treated MCF-7 cells resulted in 14 ± 0.1 DNA-PKcs-pThr2609 foci per cell, which was reduced to 3 ± 1 foci per cell after Nu7026 coadministration (Fig. 3*D*). ATM-pSer1981 foci were not altered after Nu7026 and β-lap treatment versus β-lap alone (5 ± 3 versus 5 ± 0.7, respectively), indicating that DNA-PKcs was the predominate PI3K inhibited after treatment with Nu7026 (Fig. 3*D*).

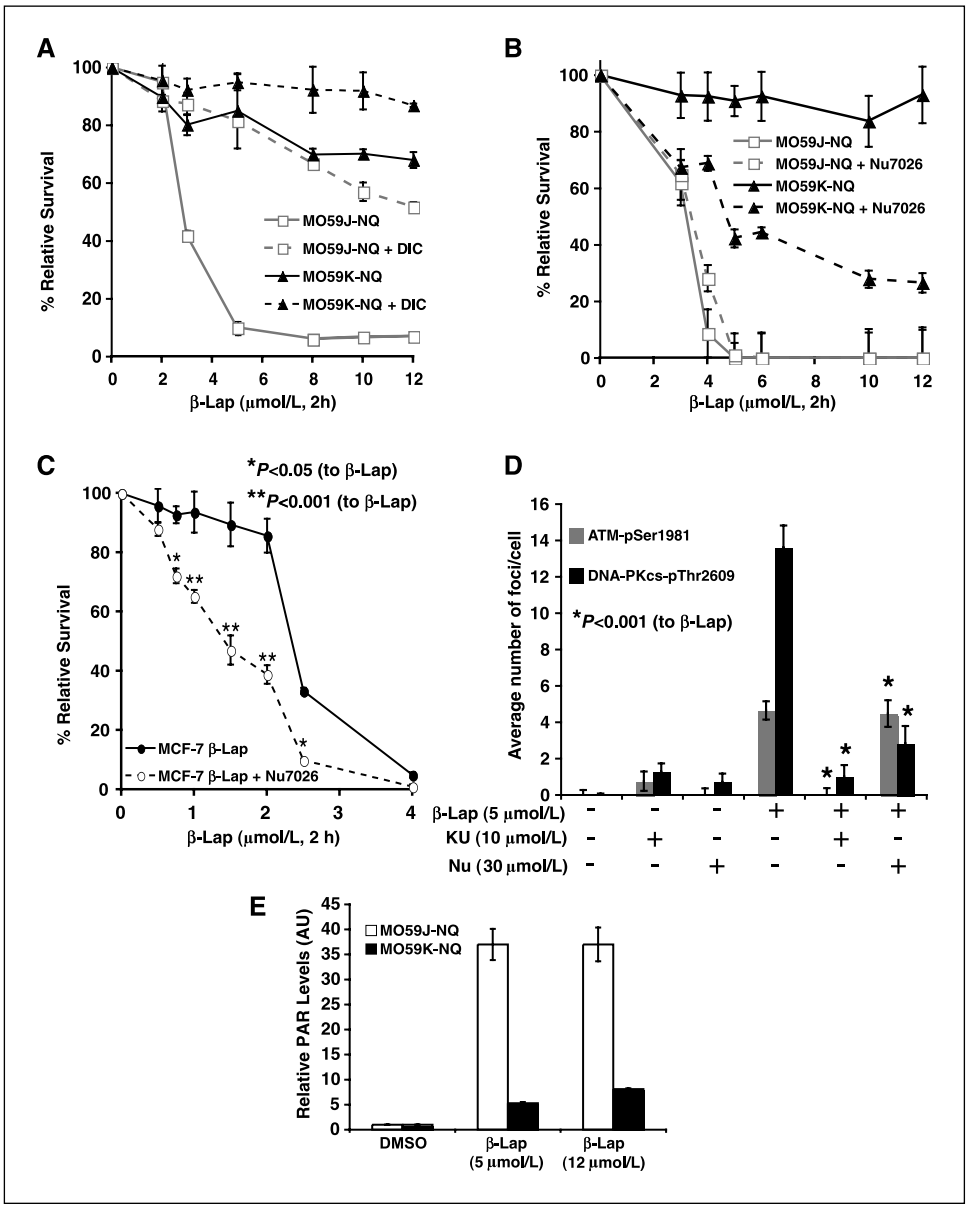

Figure 3. Loss of DNA-PKcs activity potentiates β-lap–induced cell death. *A* to *C,* cell death was examined using relative survival assays in NQO1-containing cells. *A,* MO59K-NQ$^+$ (DNA-PKcs positive) and MO59J-NQ$^+$ (DNA-PKcs negative) cells were treated with varying doses of β-lap alone or in combination with 40 μmol/L dicoumarol (*DIC*) for 2 h. After drug exposure, media were removed and drug-free medium was added. Cells were then allowed to grow for an additional 6 d and relative survival, based on DNA content, was determined by Hoechst 33258 staining as described in Materials and Methods. *B,* loss of DNA-PKcs kinase activity sensitizes MO59K-NQ$^+$ cells to β-lap. Relative survival assays using MO59K-NQ$^+$ and MO59J-NQ$^+$ pretreated and cotreated with the DNA-PKcs inhibitor Nu7026 (10 μmol/L) for 1 h before treatment with varying doses of β-lap for 2 h. *C,* inhibition of DNA-PKcs with Nu7026 potentiates β-lap–induced cell death in NQO1$^+$ MCF-7 cells. MCF-7 cells were treated with sublethal to lethal doses of β-lap alone with or without pretreatment and cotreatment with 30 μmol/L Nu7026 for 2 h. Differences were compared using two-tailed Student's *t* test. Groups having *$P \leq 0.05$ and **$P \leq 0.001$ values compared with β-lap alone are indicated. *D,* Nu7026 inhibits DNA-PKcs-pThr2609 but not ATM-pSer1981. MCF-7 cells were treated with 5 μmol/L β-lap with or without pretreatment and cotreatment with 30 μmol/L Nu7026 for 30 min. After treatment, cells were fixed and probed with antibodies to DNA-PKcs-pThr2609 and ATM-pSer1981 and foci were visualized by confocal microscopy. Quantitation of the average number of foci per cell for at least 60 cells per treatment group. *Columns,* mean; *bars,* SE. Student's *t* test for paired samples, experimental groups containing β-lap + KU55933 (*KU*) or Nu7026 (*NU*) versus β-lap alone. *, $P < 0.001$. *E,* lack of DNA-PKcs causes PARP-1 hyperactivation after β-lap treatment. Immunoblot analyses of PAR and α-tubulin protein levels from whole-cell extracts from MO59J-NQ$^+$ and MO59K-NQ$^+$ cells that were mock treated or treated with 5 or 12 μmol/L β-lap and harvested after 30 min. Relative PAR levels were determined by densitometry analyses using α-tubulin loading controls by NIH ImageJ wherein controls were set to 1.0. *Columns,* means; *bars,* SE. *AU,* arbitrary units.

We previously showed that β-lap–induced cell death was mediated by PARP-1 hyperactivation (18). Because a deficiency in DNA-PKcs potentiated β-lap–induced cell death, we examined whether NHEJ inhibition was accompanied by PARP-1 hyperactivation at sublethal doses of β-lap. PARP-1 is associated with both SSB and DSB repair. After binding to DNA breaks, PARP-1 converts β-NAD$^+$ into polymers of branched or linear poly(ADP-ribose) (PAR) units and attaches them to various nuclear proteins, including PARP-1 itself as part of its autoregulation (36). MO59J-NQ$^+$ and MO59K-NQ$^+$ cells were treated with various doses of β-lap and cell extracts prepared at 20 min posttreatment. Lethal doses of β-lap in MO59J-NQ$^+$ cells resulted in

considerable PAR accumulation, whereas the same dose that was nontoxic to MO59K-NQ$^+$ cells resulted in little PAR accumulation (Fig. 3*E*). Increasing levels of PAR polymers were noted in the MO59K-NQ$^+$ cells with increasing (≥5 μmol/L) β-lap doses (Fig. 3*E*). Treatment of β-lap-exposed MCF-7 cells with Nu7026, but not with the ATM and ATR inhibitors (KU55933 and AAI), resulted in PAR formation (data not shown).

HR-associated PI3K ATM is not necessary for β-lap–induced cell death. Because ATM autophosphorylation was observed after β-lap treatment in NQO1-proficient cancer cells, we investigated whether loss of ATM would alter β-lap–mediated lethality. Isogenic NQO1$^+$ human immortalized fibroblasts from A-T patients deficient in ATM (ATM$^{-/-}$) or proficient via ectopic ATM expression (ATM$^{+/+}$) were used (22). ATM$^{+/+}$ and ATM$^{-/-}$ cells were mock treated or exposed to various β-lap doses with or without dicoumarol for 4 h. There was no observable difference in β-lap–induced lethality between NQO1-proficient ATM$^{+/+}$ or ATM$^{-/-}$ cells, and both cells were protected from lethality by dicoumarol (Fig. 4*A*).

To corroborate these findings, MCF-7 cells were mock treated or exposed to various doses of β-lap in the presence or absence of the ATM kinase inhibitor, KU55933, or the general ATM/ATR inhibitor, AAI, for 2 or 4 h (37). KU55933 inhibited ATM-pSer1981 after β-lap or IR treatments, but did not inhibit NQO1 (Fig. 3*D*; data not shown). Although weak ATM activation was observed after sublethal doses of β-lap, inhibition of ATM by KU55933 or AAI had little effect on β-lap–induced lethality of Figs. 2*A* and 4*B–C*.

ATR activation after β-lap exposure. HR can also be mediated by ATR, which is recruited to ssDNA regions, arising due to replication fork arrest or during the processing of bulky lesions, such as UV photoproducts (38). We reasoned that β-lap could generate ROS-induced SSBs, causing replication fork stalling. Thus, we examined whether ATR activation occurred in response to β-lap by using a set of stable cell lines derived from U2OS cells (human osteosarcoma). These cells are wild-type for p53, have an intact G_1 DNA-damage checkpoint, and allow the doxycycline-inducible expression of either wild-type ATR or a dominant-negative (kinase-dead) ATR point mutant (21). ATR activation was confirmed by monitoring Chk1-pSer345 levels in WT U2OS cells after exposure to UVC or β-lap (Fig. 5*A*). Chk1-pSer345 was muted in U2OS KD-ATR cells after either UVC or β-lap exposures (Fig. 5*A*). Importantly, neither expression of WT ATR or inhibition of ATR by KD-ATR affected the survival of NQO1$^+$ U2OS cells after β-lap exposure (Fig. 5*B*). Administration of dicoumarol abrogated β-lap–induced lethality in both cell lines (Fig. 5*B*).

To confirm our findings that HR was not necessary for β-lap–induced cell death, we treated MCF-7 cells with AAI, an inhibitor of both ATM and ATR, before β-lap exposure. Inhibition of both enzymes was not sufficient to enhance β-lap–mediated cytotoxicity compared with the 80% enhancement observed after inhibition of DNA-PKcs (Figs. 3*C* and 4*C*). These data indicate that ATR signaling is activated after β-lap exposure, but that it is not a predominant factor required for survival.

β-Lap–induced ATR activation and PARP-1 hyperactivation suggested that this compound caused extensive SSBs, whereas MRN, ATM, and DNA-PK foci formation indicated delayed DSB formation. Neutral and alkaline comet assays were done to

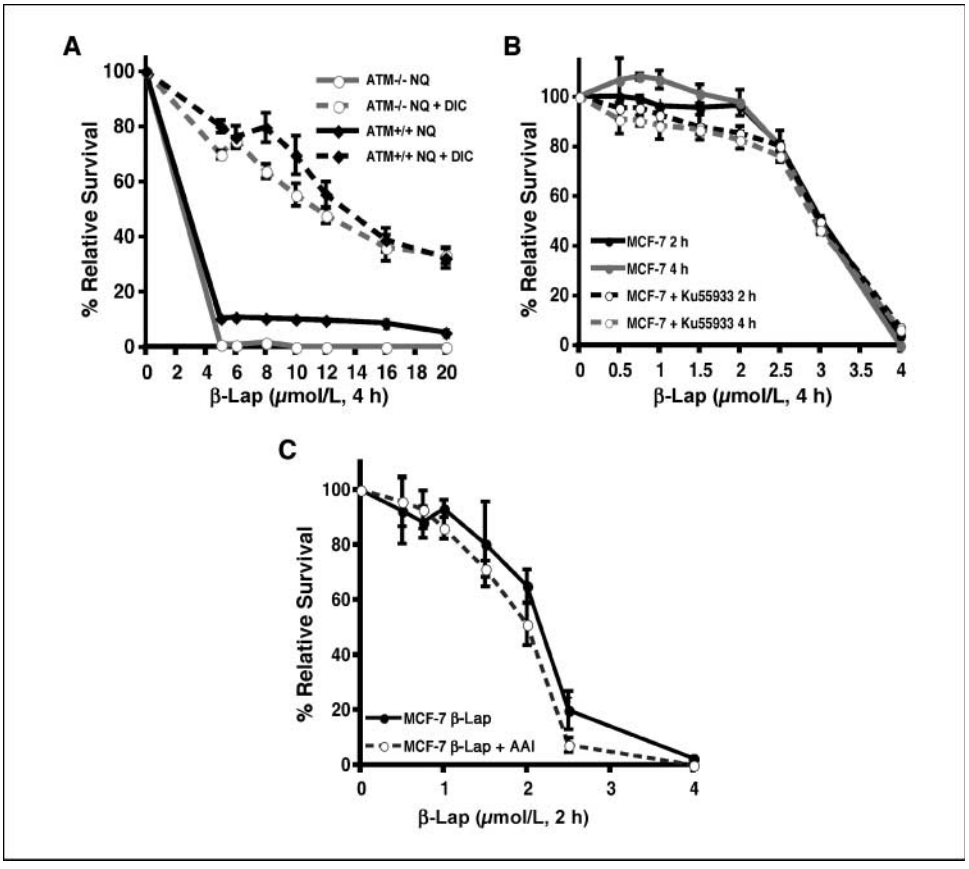

Figure 4. β-Lap–induced cell death is not dependent on ATM. *A* to *C*, cell death was monitored using relative survival assays in NQO1$^+$ cells. *A*, loss of ATM does not potentiate β-lap–induced cell death. NQO1-proficient ATM$^{-/-}$ and ATM$^{+/+}$ cells were treated with varying doses of β-lap alone or in combination with 40 μmol/L dicoumarol for 4 h. MCF-7 cells were treated with 0 to 4 μmol/L β-lap alone or with pretreatment and cotreatment with the ATM kinase inhibitor KU55933 (10 μmol/L) for 2 or 4 h (*B*) or the ATM and ATR kinase inhibitor AAI (10 μmol/L) for 2 h (*C*).

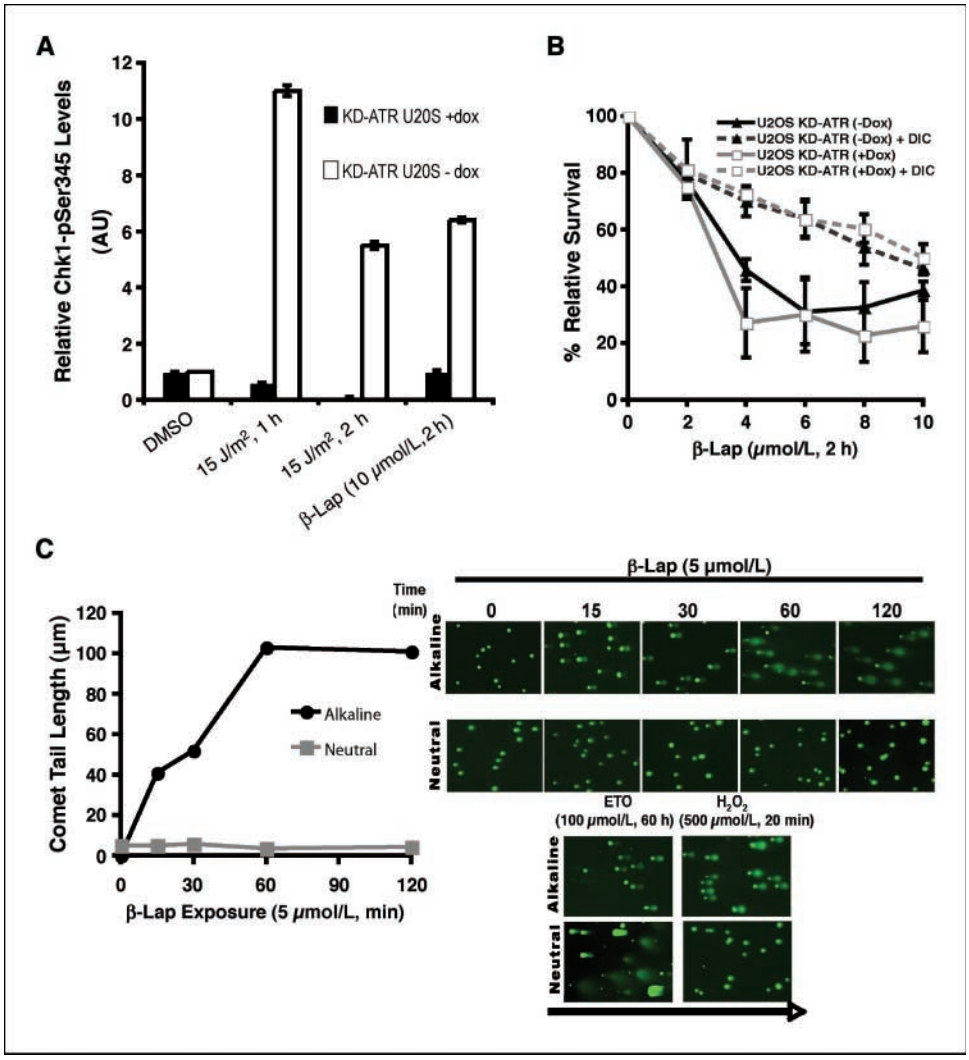

Figure 5. β-Lap causes ATR activation and SSBs. *A,* Chk1-pSer345 occurs after β-lap treatment. Immunoblots of Chk1-pSer345 and α-tubulin protein levels from whole-cell extracts of U2OS KD-ATR treated with or without 1 μg/mL doxycycline for 48 h before treatment with 10 μmol/L β-lap or 15 J/m^2 UVC. Cells were harvested at the indicated times after treatment. Relative Chk1-pSer345 levels were calculated by densitometric analyses by NIH ImageJ using α-tubulin, wherein controls were set to 1.0. *Columns,* means; *bars,* SE. *B,* KD-ATR does not alter cell death caused by β-lap. U2OS KD-ATR cells were treated with or without 1 μg/mL doxycycline (*Dox*) for 48 h to induce expression of the doxycylin-inducible kinase-dead ATR before treatment with varying doses of β-lap alone or in combination with 40 μmol/L dicoumarol for 2 h. *C,* β-lap causes formation of DNA SSBs as shown by comet assays under alkaline and neutral conditions. MCF-7 cells were treated with 5 μmol/L β-lap for 0 to 120 min. At the indicated times during drug treatment, cells were harvested for comet tail formation under either alkaline or neutral conditions. Quantified comet tail lengths of 100 cells for each time and condition calculated using NIH ImageJ software. *Points,* mean; *bars,* SE. *Arrow,* direction of electrophoresis. Not shown: 100 μmol/L etoposide (*ETO*) for 60 h under neutral and alkaline conditions had a comet tail length of roughly 81 ± 4 versus 64 ± 1 μm, respectively.

elucidate the type(s) of breaks created in NQO1-proficient human cancer cells after β-lap exposure. Sublethal doses of β-lap resulted in no detectable DNA strand breakage over time, consistent with their survival (Supplementary Fig. S3; ref. 18). In contrast, lethal doses of β-lap resulted in significant total DNA breaks, occurring immediately after drug exposure at levels surpassing breaks created after 500 μmol/L H_2O_2 (Fig. 5*C*). Prior data showed that ROS formation and DNA damage were detected within ≤5 min after β-lap addition (18). The amount of DNA strand breaks increased over time after 5 μmol/L β-lap treatment, suggesting that the lethal event may be related to the total amount of DNA breaks generated.[5] Interestingly, when cells were analyzed using neutral conditions, little to no DSBs were detected, in contrast to etoposide (ETO) treatment (Fig. 5*C*). As expected, H_2O_2 treatment caused few DSBs, similar to damage observed after β-lap exposure (Fig. 5*C*). The formation of DNA breaks after β-lap treatment was NQO1-dependent because dicoumarol prevented damage (18). These studies indicate that the majority of DNA damage caused by the NQO1-mediated metabolism of β-lap was SSBs, consistent with the genesis of "long-lived" ROS (e.g., H_2O_2).

Discussion

β-Lap, a natural product-based antitumor agent, elicits a unique cell death pathway selectively in cancer cells that express elevated NQO1 levels. The drug is currently in phase I/II clinical trials for the treatment of pancreatic as well as other cancers.[4] We recently showed that β-lap–induced cell death was dependent on PARP-1 hyperactivation, but not on typical apoptotic mediators, such as p53, Bax/Bak or caspases (17). Data from others suggested that β-lap does not cause DNA damage (39). However, we recently showed that β-lap–induced cell death was initiated by the NQO1-dependent generation of ROS, subsequent formation of DNA damage, and calcium-dependent PARP-1 hyperactivation. Once stimulated, PARP-1 hyperactivation depletes ATP/NAD^+ pools inhibiting DNA repair. Therefore, once a threshold level of DNA breaks are formed, PARP-1 hyperactivation appears to be the dominant factor, dictating downstream events leading to cell death (Fig. 6*A*; ref. 18). Because reaching the threshold level of DNA breaks required to hyperactivate PARP-1 is critical for the lethality of this drug, understanding the mechanism(s) by which cells resist

[5] K.E. Reinicke, et al. NAD(P)H:quinone oxidoreductase 1–dependent reactive oxygen species are necessary, but not sufficient, for β-lapachone–mediated cell death, submitted.

this threshold (e.g., amplified DNA repair) is important for improving its efficacy.

To determine the repair pathways activated by β-lap, we examined a number of proteins involved in DSB repair, due to their very rapid and specific localization and modification at DSBs (10). We noted delayed, β-lap–induced MRN complex activation and DNA damage with respect to IR (Figs. 1*A* and *B* and 5; Supplementary Fig. S1). Simultaneously, we noted the activation of ATM and DNA-PK as monitored by their autophosphorylation products, which only occurred in NQO1-expressing cells (Figs. 2*A–C*; Supplementary Fig. S4). Although low levels of γ-H2AX and DNA-PKcs-pThr2609 foci were evident in NQO1-deficient cells, this may be due to the metabolism of this quinone by one-electron oxidoreductases, such as NADPH cytochrome P-450 or b5R reductases (40). Overall, however, these data support a role for NQO1 in amplifying the lethal effects of β-lap via its two-electron oxidoreduction (Supplementary Fig. S4). Activation of ATM, DNA-PK, and the MRN complex were dose-dependent (Figs. 1 and 2). Evidence from our laboratory suggested that this may be due to a minimal threshold of DNA damage created after β-lap treatment, after which point the cell is committed to death via PARP-1 hyperactivation.[5]

DNA-PKcs plays a direct role in DSB repair by acting as a key component of NHEJ because defects in kinase activity result in radiosensitivity (34). Because NHEJ is the primary mechanism by which mammalian cells repair DSBs, we tested the hypothesis that NHEJ was not only activated after β-lap treatment, but necessary to protect cells from β-lap–induced lethality at sublethal doses. We noted an ~2-fold increase in the number of DNA-PKcs-pThr2609 versus ATM-pSer1981–induced foci after β-lap exposure (Fig. 2*C*). Further examination of MO59K-NQ$^+$ and MO59J-NQ$^+$ cells revealed that NHEJ was essential for survival of cells after β-lap treatment (Fig. 3*A*). Importantly, cotreatment of cells with β-lap + Nu7026, a DNA-PKcs inhibitor, sensitized MO59K-NQ$^+$ cells as well as MCF-7 cells (Fig. 3*B* and *C*), indicating a major role for NHEJ in repair of β-lap–induced DNA damage.

To determine if NHEJ inhibition enhanced PARP-1–mediated cell death at otherwise sublethal β-lap doses, we examined PAR accumulation in MO59J-NQ$^+$ and MO59K-NQ$^+$ cells. In DNA-PKcs–deficient MO59J-NQ$^+$ cells, doses of β-lap ≥5 μmol/L alone caused significant PAR modification (Fig. 3*E*). However, the proficiency of NHEJ in MO59K-NQ$^+$ cells muted PAR accumulation, consistent with its role as a cellular resistance factor in β-lap–induced lethality (Fig. 3*E*). Coadministration of Nu7026 in MCF-7 cells converted sublethal β-lap doses into a cytotoxic event accompanied by the accumulation of PAR polymers not seen with ATM or ATR inhibitors (Figs. 3*C* and 4*B* and *C*; and data not shown). These data indicate that interruption of NHEJ during β-lap treatment commits cells to PARP-1–mediated cell death (Fig. 6; ref. 18). A relationship between DNA-PK and PARP-1 has been established, and inhibition of both proteins increased net DSB over time after chemically induced damage (41, 42). Thus, combining β-lap and NHEJ inhibitors would be an ideal "two-hit" cancer therapy, by inhibiting mechanistically diverse DNA repair enzymes and thereby retarding DSB rejoining.

In addition to DNA-PKcs-pThr2609, ATM-pSer1981 was also noted after β-lap treatment (Fig. 2*A*). Although there is some discrepancy as to the exact role ATM plays in HR, it does play a pivotal role in general damage signaling, cell cycle regulation, and the slow component of DSB repair (43–45). After IR, A-T cells fail to show recovery from damage, and experiments using reverse genetics failed to see potentiation in cell death arising from the conditional loss of RAD54 in ATM$^{-/-}$ cells, suggesting an inherent HR defect in ATM$^{-/-}$ cells (46). An interplay between ATM and DNA-PKcs may be important for the proper initiation of DSB signaling and processing of DSBs to ensure repair and maintenance of genomic integrity after damage (47). Using cells deficient in ATM, we tested whether the loss of ATM, and therefore, HR-mediated repair, would alter β-lap–mediated cell death similar to that observed with NHEJ loss. Data from our studies revealed no significant difference between ATM$^{+/+}$ and ATM$^{-/-}$ cells in terms of β-lap sensitivity (Fig. 4*A*). Studies using KU55933 corroborated these findings, as inhibition of ATM did not augment lethality in β-lap–treated MCF-7 cells (Fig. 4*B*). The dose of KU55933 used in these studies was sufficient to inhibit ATM-pSer1981 after IR or β-lap–induced DNA damage (Fig. 3*D*). Interestingly, inhibition of ATM-pSer1981 by this inhibitor also abrogated DNA-PKcs-pThr2609, as recently noted by Chen et al. (47), supporting a role for ATM in DNA-PKcs-pThr2609 in response to DNA damage (Fig. 3*D*). In contrast, inhibition of

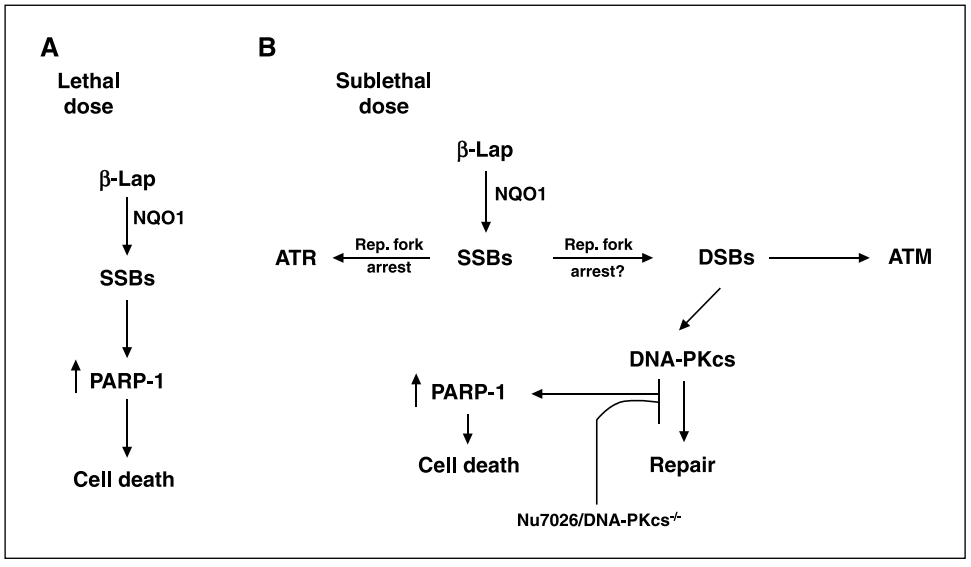

Figure 6. Model of β-lap–induced cell death after lethal and sublethal doses. *A,* β-lap–induced cell death at lethal doses is PARP-1 dominated. β-Lap–mediated metabolism by NQO1 generates ROS that cause SSBs. Extensive SSBs cause hyperactivation of PARP-1 and subsequent NAD$^+$ and ATP loss, which inhibits DNA repair and causes cell death. *B,* nonlethal doses of β-lap are converted to lethal events via DNA-PK inhibition. At sublethal doses of compound, repairable amounts of SSBs are generated, some of which may be converted to DSBs possibly via replication fork arrest. This causes the activation of members of the PI3K family of kinases, ATM, ATR, and DNA-PKcs. However, only NHEJ seems to be the primary repair pathway needed to resolve DSBs after drug treatment, as only inhibition of DNA-PKcs by either chemical (Nu7026) or genetic (DNA-PKcs$^{-/-}$) means potentiated the toxicity of sublethal doses of β-lap leading to PARP-1–mediated cell death.

DNA-PKcs with Nu7026 blocked ATM-mediated DNA-PKcs-pThr2609 (Fig. 3*D*). These data suggested that ATM-mediated DNA-PKcs-pThr2609 was a component of an amplification scheme, whereby autophosphorylation of DNA-PKcs at Thr2609 was required before signal amplification via ATM.

ATR is recruited by ATR-interacting protein to replication protein A–coated ssDNA that accumulates at stalled DNA replication forks or is generated by processing initial DNA damage (28). Thus, ATR activation in response to β-lap exposure may be consistent with stalled replication forks and could indicate the formation of DSBs from SSBs in response to β-lap exposure (48, 49). The primary lesions generated after β-lap exposure were SSBs (Fig. 5*C*). The lack of detectable DSBs could be the result of the low sensitivity of neutral comet assays compared with γ-H2AX–induced foci formation to detect minor DSBs populations. Importantly, formation of γ H2AX, as well as activation of MRN, ATM, DNA PK, and ATR appeared in a delayed manner with respect to initial SSBs (<5 min versus 10–15 min, respectively; ref. 18). These data support the hypothesis that DSBs are formed as a secondary DNA lesion after initial SSBs were generated, likely resulting from stalled replication forks (Fig. 6).

Nevertheless, ATR signaling does not seem to be a factor in β-lap resistance. Using U2OS KD-ATR and WT-ATR, we showed an increase in Chk1-pSer345 after UVC, as well as after β-lap treatment, that was muted in the presence of doxycycline, which increased dominant-negative ATR expression (Fig. 5*A*). Total levels of Chk1 and NQO1 were relatively unchanged under doxycycline treatment (data not shown). U2OS KD-ATR cells treated with or without doxycycline showed no enhanced β-lap toxicity (Fig. 5*B*). Furthermore, addition of AAI had no apparent effect on β-lap–induced cytotoxicity in MCF-7 cells (Fig. 4*C*). Thus, neither ATM nor ATR seem to play major roles as resistance factors in β-lap lethality.

Currently used cancer chemotherapeutic agents function primarily as nonselective inducers of DSBs in highly proliferative cells. A major problem with many of these agents is their lack of selectivity, in which both normal and cancerous tissues are targeted. In contrast, β-lap, which is currently under investigation in phase I/II clinical trials, selectively targets cancer cells that express elevated NQO1 levels, resulting in DNA damage and cell death mediated by PARP-1 (18). Here, we show that in addition to SSB-induced DNA repair pathways, β-lap activates various DSB repair pathways. In particular, NHEJ was a key factor in the survival of cells exposed to β-lap, because inhibition of NHEJ causes PARP-1–mediated cell death after treatment or sublethal doses of β-lap. In summary, these data warrant the combinatorial use of β-lap with inhibitors of NHEJ thereby increasing the therapeutic efficacy of this compound by targeting two distinct repair mechanisms, NHEJ and PARP-1.

Acknowledgments

Received 3/12/2007; accepted 5/8/2007.

Grant support: NIH/National Cancer Institute grant CA10279201 (D.A. Boothman), CWRU Core grant P30CA43703-12, and Department of Defense Breast Cancer Program Predoctoral Fellowships W81XWH-04-1-0301 (M.S. Bentle) and W81XWH-05-1-0248 (K.E. Reinicke).

The costs of publication of this article were defrayed in part by the payment of page charges. This article must therefore be hereby marked *advertisement* in accordance with 18 U.S.C. Section 1734 solely to indicate this fact.

References

1. Krasin F, Hutchinson F. Repair of DNA double-strand breaks in *Escherichia coli*, which requires recA function and the presence of a duplicate genome. J Mol Biol 1977;116:81–98.
2. D'Andrea AD, Haseltine WA. Modification of DNA by aflatoxin B1 creates alkali-labile lesions in DNA at positions of guanine and adenine. Proc Natl Acad Sci U S A 1978;75:4120–4.
3. Kuzminov A. Single-strand interruptions in replicating chromosomes cause double-strand breaks. Proc Natl Acad Sci U S A 2001;98:8241–6.
4. Rich T, Allen RL, Wyllie AH. Defying death after DNA damage. Nature 2000;407:777–83.
5. van Gent DC, Hoeijmakers JH, Kanaar R. Chromosomal stability and the DNA double-stranded break connection. Nat Rev Genet 2001;2:196–206.
6. Richardson C, Jasin M. Coupled homologous and nonhomologous repair of a double-strand break preserves genomic integrity in mammalian cells. Mol Cell Biol 2000;20:9068–75.
7. Khanna KK, Jackson SP. DNA double-strand breaks: signaling, repair and the cancer connection. Nat Genet 2001;27:247–54.
8. Rogakou EP, Pilch DR, Orr AH, Ivanova VS, Bonner WM. DNA double-stranded breaks induce histone H2AX phosphorylation on serine 139. J Biol Chem 1998;273:5858–68.
9. Foster ER, Downs JA. Histone H2A phosphorylation in DNA double-strand break repair. FEBS J 2005;272:3231–40.
10. Paull TT, Rogakou EP, Yamazaki V, Kirchgessner CU, Gellert M, Bonner WM. A critical role for histone H2AX in recruitment of repair factors to nuclear foci after DNA damage. Curr Biol 2000;10:886–95.
11. Chowdhury D, Keogh MC, Ishii H, Peterson CL, Buratowski S, Lieberman J. γ-H2AX dephosphorylation by protein phosphatase 2A facilitates DNA double-strand break repair. Mol Cell 2005;20:801–9.
12. Jackson SP. Sensing and repairing DNA double-strand breaks. Carcinogenesis 2002;23:687–96.
13. Trujillo KM, Yuan SS, Lee EY, Sung P. Nuclease activities in a complex of human recombination and DNA repair factors Rad50, Mre11, and p95. J Biol Chem 1998;273:21447–50.
14. Pink JJ, Planchon SM, Tagliarino C, Varnes ME, Siegel D, Boothman DA. NAD(P)H:quinone oxidoreductase activity is the principal determinant of β-lapachone cytotoxicity. J Biol Chem 2000;275:5416–24.
15. Boothman DA, Pardee AB. Inhibition of radiation-induced neoplastic transformation by β-lapachone. Proc Natl Acad Sci U S A 1989;86:4963–7.
16. Suzuki M, Amano M, Choi J, et al. Synergistic effects of radiation and β-lapachone in DU-145 human prostate cancer cells *in vitro*. Radiat Res 2006;165:525–31.
17. Bentle MS, Bey EA, Dong Y, Reinicke KE, Boothman DA. New tricks for old drugs: the anticarcinogenic potential of DNA repair inhibitors. J Mol Histol 2006;37:203–18.
18. Bentle MS, Reinicke KE, Bey EA, Spitz DR, Boothman DA. Calcium-dependent modulation of poly(ADP-ribose) polymerase-1 alters cellular metabolism and DNA repair. J Biol Chem 2006;281:33684–96.
19. Wuerzberger SM, Pink JJ, Planchon SM, Byers KL, Bornmann WG, Boothman DA. Induction of apoptosis in MCF-7:WS8 breast cancer cells by β-lapachone. Cancer Res 1998;58:1876–85.
20. Lees-Miller SP, Godbout R, Chan DW, et al. Absence of p350 subunit of DNA-activated protein kinase from a radiosensitive human cell line. Science 1995;267:1183–5.
21. Nghiem P, Park PK, Kim Ys YS, Desai BN, Schreiber SL. ATR is not required for p53 activation but synergizes with p53 in the replication checkpoint. J Biol Chem 2002;277:4428–34.
22. Ziv Y, Bar-Shira A, Pecker I, et al. Recombinant ATM protein complements the cellular A-T phenotype. Oncogene 1997;15:159–67.
23. Patton JT, Mayo LD, Singhi AD, Gudkov AV, Stark GR, Jackson MW. Levels of HdmX expression dictate the sensitivity of normal and transformed cells to Nutlin-3. Cancer Res 2006;66:3169–76.
24. Pink JJ, Wuerzberger-Davis S, Tagliarino C, et al. Activation of a cysteine protease in MCF-7 and T47D breast cancer cells during β-lapachone-mediated apoptosis. Exp Cell Res 2000;255:144–55.
25. Boothman DA, Meyers M, Fukunaga N, Lee SW. Isolation of X-ray-inducible transcripts from radioresistant human melanoma cells. Proc Natl Acad Sci U S A 1993;90:7200–4.
26. Siegel D, Franklin WA, Ross D. Immunohistochemical detection of NAD(P)H:quinone oxidoreductase in human lung and lung tumors. Clin Cancer Res 1998;4:2065–70.
27. Menacho-Marquez M, Murguia JR. β-lapachone activates a Mre11p-Tel1p G1/S checkpoint in budding yeast. Cell Cycle 2006;5:2509–16.
28. Kurz EU, Lees-Miller SP. DNA damage-induced activation of ATM and ATM-dependent signaling pathways. DNA Repair (Amst) 2004;3:889–900.
29. Rothkamm K, Lobrich M. Evidence for a lack of DNA double-strand break repair in human cells exposed to very low X-ray doses. Proc Natl Acad Sci U S A 2003;100:5057–62.
30. Winski SL, Koutalos Y, Bentley DL, Ross D. Subcellular localization of NAD(P)H:quinone oxidoreductase 1 in human cancer cells. Cancer Res 2002;62:1420–4.
31. Bakkenist CJ, Kastan MB. DNA damage activates ATM through intermolecular autophosphorylation and dimer dissociation. Nature 2003;421:499–506.
32. Chan DW, Chen BP, Prithivirajsingh S, et al. Autophosphorylation of the DNA-dependent protein kinase catalytic subunit is required for rejoining of DNA double-strand breaks. Genes Dev 2002;16:2333–8.

33. Ding Q, Reddy YV, Wang W, et al. Autophosphorylation of the catalytic subunit of the DNA-dependent protein kinase is required for efficient end processing during DNA double-strand break repair. Mol Cell Biol 2003;23:5836–48.

34. Allalunis-Turner MJ, Barron GM, Day RS III, Dobler KD, Mirzayans R. Isolation of two cell lines from a human malignant glioma specimen differing in sensitivity to radiation and chemotherapeutic drugs. Radiat Res 1993;134:349–54.

35. Veuger SJ, Curtin NJ, Richardson CJ, Smith GC, Durkacz BW. Radiosensitization and DNA repair inhibition by the combined use of novel inhibitors of DNA-dependent protein kinase and poly(ADP-ribose) polymerase-1. Cancer Res 2003;63:6008–15.

36. Kim MY, Zhang T, Kraus WL. Poly(ADP-ribosyl)ation by PARP-1: "PAR-laying" NAD+ into a nuclear signal. Genes Dev 2005;19:1951–67.

37. Hickson I, Zhao Y, Richardson CJ, et al. Identification and characterization of a novel and specific inhibitor of the ataxia-telangiectasia mutated kinase ATM. Cancer Res 2004;64:9152–9.

38. Cortez D, Guntuku S, Qin J, Elledge SJ. ATR and ATRIP: partners in checkpoint signaling. Science 2001;294:1713–6.

39. Pardee AB, Li YZ, Li CJ. Cancer therapy with β-lapachone. Curr Cancer Drug Targets 2002;2:227–42.

40. Byczkowski JZ, Gessner T. Inhibition of the redox cycling of vitamin K3 (menadione) in mouse liver microsomes. Int J Biochem 1988;20:1073–9.

41. Boulton S, Kyle S, Durkacz BW. Interactive effects of inhibitors of poly(ADP-ribose) polymerase and DNA-dependent protein kinase on cellular responses to DNA damage. Carcinogenesis 1999;20:199–203.

42. Ruscetti T, Lehnert BE, Halbrook J, et al. Stimulation of the DNA-dependent protein kinase by poly(ADP-ribose) polymerase. J Biol Chem 1998;273:14461–7.

43. Kuhne M, Riballo E, Rief N, Rothkamm K, Jeggo PA, Lobrich M. A double-strand break repair defect in ATM-deficient cells contributes to radiosensitivity. Cancer Res 2004;64:500–8.

44. Riballo E, Kuhne M, Rief N, et al. A pathway of double-strand break rejoining dependent upon ATM, Artemis, and proteins locating to γ-H2AX foci. Mol Cell 2004;16:715–24.

45. Shiloh Y. The ATM-mediated DNA-damage response: taking shape. Trends Biochem Sci 2006;31:402–10.

46. Morrison C, Sonoda E, Takao N, Shinohara A, Yamamoto K, Takeda S. The controlling role of ATM in homologous recombinational repair of DNA damage. EMBO J 2000;19:463–71.

47. Chen BP, Uematsu N, Kobayashi J, et al. ATM is essential for DNA-pkcs phosphorylations at T2609 cluster upon DNA double strand break. J Biol Chem 2006;282:6582–7.

48. Michel B, Ehrlich SD, Uzest M. DNA double-strand breaks caused by replication arrest. EMBO J 1997;16:430–8.

49. Michel B, Grompone G, Flores MJ, Bidnenko V. Multiple pathways process stalled replication forks. Proc Natl Acad Sci U S A 2004;101:12783–8.